

1 **Re-evaluating the reactive uptake of HOBr in the troposphere with**  
2 **implications for the marine boundary layer and volcanic plumes**

3

4 **Tjarda J. Roberts<sup>1</sup>, Line Jourdain<sup>1</sup>, Paul T. Griffiths<sup>2</sup>, and Michel Pirre<sup>1</sup>**

5

6 [1] {LPC2E, UMR 7328, CNRS-Université d'Orléans, 3A Avenue de la Recherche  
7 Scientifique, 45071 Orleans, Cedex 2, France}

8 [2] {Centre for Atmospheric Science, Cambridge University, Chemistry Department,  
9 Lensfield Road, Cambridge, CB2 1EW, UK}

10

11 Correspondence to: T. J. Roberts (Tjarda.Roberts@cnsr-orleans.fr)

12

13

14 **Abstract**

15 The reactive uptake of HOBr onto halogen-rich aerosols promotes conversion of  $\text{Br}^-_{(\text{aq})}$  into gaseous  
16 reactive bromine (incl. BrO) with impacts on tropospheric oxidants and mercury deposition.  
17 However, experimental data quantifying HOBr reactive uptake on tropospheric aerosols is limited,  
18 and reported values vary in magnitude. This study introduces a new evaluation of HOBr reactive  
19 uptake coefficients in the context of the general acid assisted mechanism. We emphasise that the  
20 termolecular kinetic approach assumed in numerical model studies of tropospheric reactive bromine  
21 chemistry to date is strictly only valid for a specific pH range and, according to the general acid  
22 assisted mechanism for HOBr, the reaction kinetics becomes bimolecular and independent of pH at  
23 high acidity.

24 This study reconciles for the first time the different reactive uptake coefficients reported from  
25 laboratory experiments. The re-evaluation confirms HOBr reactive uptake is rapid on moderately  
26 acidified sea-salt aerosol (and slow on alkaline aerosol), but predicts very low reactive uptake  
27 coefficients on highly-acidified submicron particles. This is due to acid-saturated kinetics combined  
28 with low halide concentrations induced by both acid-displacement reactions and the dilution effects  
29 of  $\text{H}_2\text{SO}_{4(\text{aq})}$ . A mechanism is thereby proposed for reported Br-enhancement (relative to Na) in  
30  $\text{H}_2\text{SO}_4$ -rich submicron particles in the marine environment. Further, the fact that HOBr reactive  
31 uptake on  $\text{H}_2\text{SO}_4$ -acidified supra-micron particles is driven by  $\text{HOBr}+\text{Br}^-$  (rather than  $\text{HOBr}+\text{Cl}^-$ )  
32 indicates self-limitation via decreasing  $\gamma_{\text{HOBr}}$  once aerosol  $\text{Br}^-$  is converted into reactive bromine.

33 First predictions of HOBr reactive uptake on sulphate particles in halogen-rich volcanic plumes are  
34 also presented. High (accommodation limited)  $\text{HOBr}+\text{Br}^-$  uptake coefficient in concentrated ( $> 1$   
35  $\mu\text{mol/mol SO}_2$ ) plume environments supports potential for rapid BrO formation in plumes  
36 throughout the troposphere. However, reduced HOBr reactive uptake may reduce the rate of BrO  
37 cycling in dilute plumes in the lower troposphere.

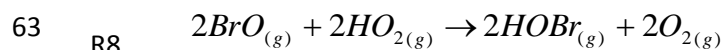
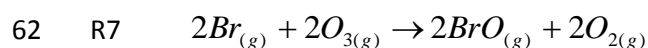
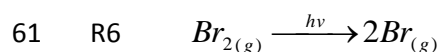
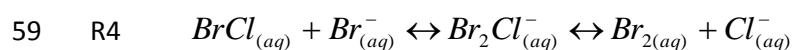
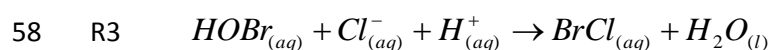
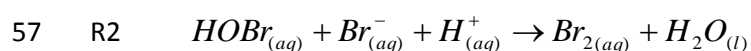
38 In summary, our re-evaluation of HOBr kinetics provides a new framework for interpretation of  
39 experimental data and suggests the reactive uptake of HOBr on  $\text{H}_2\text{SO}_4$ -acidified particles is  
40 substantially over-estimated in current numerical models of BrO chemistry in the troposphere.

41

## 42 1. Introduction

43 The reactive uptake of HOBr onto halogen-containing aerosols to release Br<sub>2</sub> enables propagation of  
44 the chain reaction leading to autocatalytic BrO formation, the so-called 'bromine explosion', (Vogt et  
45 al., 1996), first proposed following the discovery of ozone depletion events in the polar boundary  
46 layer (Barrie et al. 1988). Rapid and substantial (10's ppbv) ozone depletion occurs upon the  
47 formation of just 10's pptv BrO due to cycling between Br and BrO, with further Br-mediated impacts  
48 on environmental mercury in the conversion of Hg<sup>0</sup> to more reactive and easily deposited form Hg<sup>II</sup>  
49 (Schroeder et al., 1998). Tropospheric BrO chemistry has since been recognised outside the polar  
50 regions, with BrO identified above salt pans (Hebestreit et al., 1999), in the marine boundary layer  
51 (Read et al. 2008), and is suggested to have a significant impact on the chemistry of the free  
52 troposphere (e.g. von Glasow et al., 2004). In particular, recent evidence of rapid BrO formation in  
53 acidic volcanic plumes (10's pptv to ppbv on a timescale of minutes) has highlighted volcanic halogen  
54 emissions as a source of reactive bromine entering the troposphere (Bobrowski et al., 2003).

55



64

65 Key to reactive halogen formation is the cycle R1-R8 which results in autocatalytic formation of BrO.  
66 Accommodation of HOBr<sub>(g)</sub> to aerosol (R1), followed by reaction with Br<sub>(aq)</sub><sup>-</sup> or Cl<sub>(aq)</sub><sup>-</sup> and H<sub>(aq)</sub><sup>+</sup> results  
67 in a di-halogen product (R2,R3). The reaction of HOBr with Cl<sub>(aq)</sub><sup>-</sup> (R3) is typically considered the  
68 dominant reaction pathway (albeit an assumption that may not apply in highly acidified aerosol as

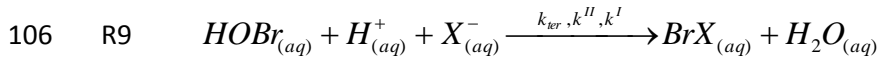
69 we show in this study) given sea-salt aerosol contains  $[\text{Br}_{(\text{aq})}^-] \ll [\text{Cl}_{(\text{aq})}^-]$  by a factor of 700 (or greater  
70 once reactive bromine formation has commenced), and the termolecular rate constants for R2 and  
71 R3 are of comparable magnitudes (Liu and Margare, 2001, Beckwith et al., 1996). However,  $\text{Br}_2$  is  
72 commonly the observed product, as confirmed by laboratory experiments by Fickert et al. (1999).  
73 The product conversion from  $\text{BrCl}$  to  $\text{Br}_2$  is explained by aqueous-phase equilibria (R4) that  
74 interconvert  $\text{BrCl}$  into  $\text{Br}_2$  (via  $\text{Br}_2\text{Cl}^-$ ) before gaseous release (R5). According to equilibrium constants  
75 reported by Wang et al. (1994), conversion of  $\text{BrCl}$  to  $\text{Br}_2$  is favoured at room temperature in aerosol  
76 provided  $\text{Br}_{(\text{aq})}^-:\text{Cl}_{(\text{aq})}^- > \sim 10^{-4}$ , as for example in sea-salt aerosol where  $\text{Br}_{(\text{aq})}^-:\text{Cl}_{(\text{aq})}^- \approx 1.5 \cdot 10^{-3}$ . The  
77 dihalogen species then partition into the gas-phase, R5. The exsolution of dihalogens from the  
78 aerosol to the gas-phase also limits the occurrence of reverse reactions that might reform HOBr.  
79 Once in the gas-phase,  $\text{Br}_2$  is photolysed to produce 2 Br radicals, R6, which may react with ozone to  
80 form BrO, R7. HOBr is reformed via the reaction of BrO with  $\text{HO}_2$ , (R8), whereupon it may react again  
81 with halogen-containing aerosol to further propagate the cycle, each time doubling the  
82 concentration of reactive bromine.

83

84 Numerical models have been developed to better understand the formation of BrO and evaluate  
85 impacts on atmospheric oxidants throughout the troposphere and on mercury cycling in the  
86 environment. Models capture the salient features of BrO formation and impacts (e.g. on ozone  
87 depletion and Hg deposition events) in the different tropospheric environments (for reviews by  
88 Simpson et al. 2007 and Saiz-Lopez A. and von Glasow R., 2012). Nevertheless, a number of  
89 uncertainties remain. For example, models tend to overestimate  $\text{Br}_x$  cycling in the marine  
90 environment (Sander et al., 2003; Smoydzin and von Glasow, 2007; Keene et al., 2009). Models  
91 predict a depletion in the inorganic bromine content of all acidified marine aerosols, as consequence  
92 of HOBr reactive uptake to form  $\text{Br}_2$  and its release into the gas-phase. However, an aerosol bromine  
93 deficit is only observed in the slightly acidified supramicron fraction, whilst aerosol bromine is found  
94 to be enhanced (relative to that expected based on  $\text{Br}:\text{Na}$  ratios in sea-salt, using sodium as a sea-  
95 salt tracer) in the highly acidified sub-micronmeter fraction. This phenomenon has not been  
96 explained to date (Sander et al., 2003). Numerical models have also attempted to simulate reactive  
97 halogen chemistry in volcanic plume environments. Models initialised with a high-temperature  
98 source region, are able to reproduce the rapid formation of BrO in the near-source plume  
99 (Bobrowski et al., 2007a, Roberts et al., 2009, Von Glasow 2010), as well as ozone depletion (Kelly et  
100 al., 2013), but a source of model uncertainty is the representation of heterogeneous halogen

101 chemistry on volcanic aerosol, which may differ from that reported from experiments on sea-salt  
102 aerosol.

103 All these studies rely on laboratory experiments to quantify rate constants of the reactions, with a  
104 key process in the formation of reactive bromine being the reaction of  $\text{HOBr}_{(aq)}$  with halide ion  $\text{X}^-_{(aq)}$   
105 ( $\text{Cl}^-_{(aq)}$  or  $\text{Br}^-_{(aq)}$ ) and  $\text{H}^+_{(aq)}$ , R2,R3, which can be written generically as R9.



107 Experimental studies (e.g. Fickert et al., 1999) show the reaction of  $\text{HOBr}_{(aq)}$  is promoted when  
108 alkaline sea-salt aerosols becomes acidified, either by natural (e.g. methane sulphonic acid) or  
109 anthropogenic (e.g. sulphuric acid) sources of acidity. However, laboratory experiments have  
110 reported uptake coefficients on acidified sea-salt aerosol,  $>0.2$  (Abbatt and Wachewsky, 1998) and  
111  $10^{-2}$  (Pratte and Rossi, 2006), a discrepancy that has not been explained to date. In addition, no  
112 experiments have been performed to quantify uptake of HOBr on volcanic aerosol under  
113 tropospheric conditions.

114 Numerical model studies of reactive bromine chemistry currently implement R9 using three-body  
115 reaction kinetics, i.e. assumed the reaction rate is directly proportional to  $\text{H}^+_{(aq)}$  concentration (e.g.  
116 von Glasow, 2002), or using uptake coefficients calculated on this assumption (see Ammann et al.,  
117 2013 and the IUPAC Task group evaluation website). We highlight, however, that earlier literature on  
118 the general acid-assisted mechanism for this and similar reactions (e.g. Eigen and Kustin, 1962, Nagy  
119 et al., 1988) identify that the pH dependence of the reaction rate is more complex, with acid-  
120 saturation of the kinetics at high acidity.

121 This study re-evaluates HOBr reactive uptake in the context of the general acid assisted mechanism  
122 for the first time. The plan of the paper is as follows. In Section 2 the method for calculating the  
123 reactive uptake coefficient is recalled with the approach based on the general acid assisted  
124 mechanism explained. The data used to evaluate the new uptake coefficient calculations are  
125 presented. In Section 3 pH-dependent second-order rate constants ( $k^{\text{II}}$ ) are derived for both  
126  $\text{HOBr} + \text{Br}^-$  and  $\text{HOBr} + \text{Cl}^-$  in the context of the general assisted mechanism, using reported literature  
127 data for the underlying rate constants, and a thermodynamic model to predict aerosol composition  
128 under experimental conditions. Using the new parameterisation for  $k^{\text{II}}$ , reactive uptake coefficients  
129 for  $\text{HOBr} + \text{Br}^-$  and  $\text{HOBr} + \text{Cl}^-$  are calculated and compared to reported laboratory data for HCl-  
130 acidified sea-salt aerosol (Wachewsky and Abbatt, 1998) and  $\text{H}_2\text{SO}_4$ -acidified sea-salt aerosol (Pratte  
131 and Rossi, 2006). We provide new quantification of  $\text{HOBr} + \text{Br}^-$  and  $\text{HOBr} + \text{Cl}^-$  uptake coefficients on  
132  $\text{H}_2\text{SO}_4$ -acidified sea-salt aerosol in the marine environment, and sulphuric acid aerosol in volcanic

133 plumes dispersing into the troposphere. In section 4, reactive uptake coefficients are calculated for  
 134 HOBr on H<sub>2</sub>SO<sub>4</sub>-acidified sea-salt aerosol in the marine environment, and on sulphuric acid aerosol in  
 135 volcanic plumes entering the troposphere, and implications discussed for BrO chemistry in these  
 136 environments.

137

## 138 2. Method and experimental data

### 139 2.1 Quantifying the reactive uptake coefficient, $\gamma_{\text{HOBr}}$

140 The reactive uptake of HOBr<sub>(g)</sub> can be quantified by E1 (with further modification required for large  
 141 particles due to the limitation of gas-phase diffusion) in terms of the reactive uptake coefficient,  
 142  $\gamma_{\text{HOBr}}$ , where  $v_{\text{HOBr}}$  is the mean molecular velocity of HOBr<sub>(g)</sub>, cm s<sup>-1</sup>, and *Area*, is the surface area  
 143 density of the aqueous phase, cm<sup>2</sup>/cm<sup>3</sup>.

144  $\gamma_{\text{HOBr}}$  is a fractional number that quantifies the likelihood of reaction given a collision of HOBr<sub>(g)</sub> with  
 145 a particle, and can be calculated following the resistor-model framework (E2) that describes the  
 146 accommodation to the aerosol, and the reaction and diffusion in or across the aerosol particle.  $\gamma_{\text{HOBr}}$   
 147 is a function of several parameters, including accommodation coefficient,  $\alpha_{\text{HOBr}}$ , the solubility of  
 148 HOBr,  $H^*$ , the aqueous-phase diffusion rate,  $D_l$ , the gas constant  $R$ , Temperature,  $T$ , the mean  
 149 molecular velocity,  $v_{\text{HOBr}}$ , and the first-order rate constant for the reaction of HOBr<sub>(aq)</sub>,  $k^I$ . The  
 150 parameter  $l$  is a function of  $D_l$  and  $k^I$ ,  $l = (D_l/k^I)^{0.5}$ .

$$151 \quad \text{E1} \quad -\frac{d[\text{HOBr}_{(g)}]}{dt} = \gamma_{\text{HOBr}} \cdot \frac{v_{\text{HOBr}}}{4} \cdot [\text{HOBr}_{(g)}] \cdot \text{Area}$$

$$152 \quad \text{E2} \quad \frac{1}{\gamma_{\text{HOBr}}} = \frac{1}{\alpha_{\text{HOBr}}} + \frac{v_{\text{HOBr}}}{4 \cdot H^*_{\text{HOBr}} \cdot R \cdot T \cdot \sqrt{D_{l,\text{HOBr}} \cdot k^I}} \cdot \frac{1}{\coth\left[\frac{r}{l}\right] - \frac{l}{r}}$$

$$153 \quad \text{E3} \quad -\frac{d[\text{HOBr}_{(aq)}]}{dt} = k^I \cdot [\text{HOBr}_{(aq)}]$$

$$154 \quad \text{E4} \quad k^I = k_{\text{ter}} \cdot [X_{(aq)}^-] \cdot [H_{(aq)}^+]$$

$$155 \quad \text{E5} \quad k^I = k^{II} \cdot [X_{(aq)}^-]$$

156 To date, numerical models have adopted two approaches to simulate the reactive uptake of HOBr.  
 157 Detailed process models (e.g. MISTRA; von Glasow et al. (2002), MECCA; Sander et al. (2011)) tend  
 158 to model HOBr gas-aerosol partitioning to and from the aerosol directly, with the reaction of HOBr

159 inside the aerosol simulated using E3 and termolecular kinetics (E4). On the other hand, global  
160 models (e.g. in studies by von Glasow et al., (2004), Yang et al., (2005), Breider et al., (2010), Parella  
161 et al. (2012)) tend to simulate HOBr reactive uptake as one step, E1, quantified by the uptake  
162 coefficient,  $\gamma_{\text{HOBr}}$ . The IUPAC evaluation recommends uptake coefficient to be calculated using E2  
163 and the termolecular approach to HOBr kinetics, E4. In global models, a fixed uptake coefficient,  
164  $\gamma_{\text{HOBr}}$ , is typically used for computational reasons.

165 However, as we highlight in this study, the termolecular kinetics approach (E4) is only valid within a  
166 limited pH range. Here we instead use E2 and the reaction kinetics of  $\text{HOBr}_{(\text{aq})}$  in terms of a second-  
167 order rate constant, E5, where  $k^{\text{II}}$  is a variable function of pH according to the general acid assisted  
168 reaction mechanism for  $\text{HOX}+\text{Y}^- (+\text{H}^+)$  constrained by available laboratory data. Details on the  
169 mechanism and derivation of  $k^{\text{II}}$  are given in Section 1 of Supplementary material and Section 3.1).  
170 Despite being well-documented (Eigen and Kustin, 1962; Kumar and Margare, 1987; Nagy et al.  
171 1988; Gerritsen and Margare, 1990, Wang and Margare, 1994) this mechanism has not been  
172 implemented in any numerical model studies of reactive halogen chemistry to date.

173 To calculate reactive uptake coefficients (E2), we also need to determine the aerosol composition,  
174 specifically halide concentration,  $[\text{X}^-_{(\text{aq})}]$  and the acidity. Indeed,  $[\text{X}^-_{(\text{aq})}]$  is needed for E5 and  
175 subsequently E2, and the acidity is also needed to determine  $k^{\text{II}}$  in the context of the general  
176 assisted mechanism (see the expression in Section 3.1) and subsequently E5 and E2. This was  
177 achieved using the E-AIM (Extended- Aerosol Inorganic model) and Henry's constants (for more  
178 details see Section 3 of Supplementary Material). Given high ionic strength of the solutions studied,  
179 concentrations were converted to activities using activity coefficients provided by E-AIM.

180 Finally, we assume in E2 an accommodation coefficient of 0.6 (Wachsmuth et al., 2002), with  
181 solubility and diffusion coefficients for HOBr in water and sulphuric acid derived from Frenzel et al.  
182 (1998), Iraci et al. (2005), and Klassen et al (1998). A radius of 0.1 or 1  $\mu\text{m}$  was assumed, reflecting  
183 the presence of both sub- and supra-micron particles in volcanic and marine environments. Further  
184 details are provided in Section 2 of Supplementary Materials.

185 We compare our new approach to reported estimates of HOBr reactive uptake coefficients from  
186 laboratory experiments as outlined below.

187

## 188 **2.2 Reported experimental studies on the reactive uptake of HOBr onto liquid aerosol**

189 A number of laboratory experiments (Table 1) have quantified the reactive uptake of HOBr onto  
190 acidified sea-salt aerosol under tropospheric conditions (as well as on solid particles, not considered

191 here). The accommodation coefficient for HOBr onto super-saturated  $\text{NaBr}_{(\text{aq})}$  aerosol was  
192 determined by Wachsumth et al. (2002) to be  $\alpha_{\text{HOBr}} = 0.6 \pm 0.2$  at 298 K.

193 Experiments using acidified sea-salt particles made by nebulizing a 5 M NaCl and 0.5 M HCl solution  
194 under conditions representative of the troposphere found the reactive uptake coefficient for the  
195 reaction ( $\text{HOBr} + \text{Cl}^-$ ) to be very high ( $\gamma_{\text{HOBr}} > 0.2$ ) on deliquesced aerosol ( $\text{RH} > 75\%$ ,  $T = 298 \text{ K}$ ),  
196 (Abbatt and Waschewsky, 1998). Conversely, experiments by Pratte and Rossi (2006) on  $\text{H}_2\text{SO}_4$ -  
197 acidified sea-salt aerosol with  $\text{H}_2\text{SO}_4:\text{NaCl}$  molar ratio = 1.45:1 at 296 K measured a substantially  
198 lower HOBr uptake coefficient,  $\gamma_{\text{HOBr}} \sim 10^{-2}$ , with a dependence on relative humidity ( $\gamma_{\text{HOBr}} \sim 10^{-3}$   
199 below 70% RH). This large ( $10^1$ - $10^2$ ) discrepancy has not been resolved to date. Uptake of HOBr on  
200 pure sulfate aerosol at 296 K is found to be low ( $\gamma_{\text{HOBr}} \sim 10^{-3}$ ), Pratte and Rossi (2006).

201 Aqueous-phase rate constants for the reaction of  $\text{HOBr} + \text{X}^- + \text{H}^+$  have also been reported: for  $\text{HOBr} + \text{Br}^-$   
202  $_{(\text{aq})}$ , Eigen and Kustin (1952) and Beckwith et al. (1996) report termolecular rate constants of  $k_{\text{ter}} =$   
203  $1.6 \cdot 10^{10} \text{ M}^{-2} \text{ s}^{-2}$  over a pH range of 2.7-3.6 and 1.9-2.4 at 298 K, respectively. For  $\text{HOBr} + \text{Cl}^-_{(\text{aq})}$ , Liu and  
204 Margarem (2001) report a three-body rate constant of  $2.3 \cdot 10^{10} \text{ M}^{-2} \text{ s}^{-2}$  in buffered aerosol at pH = 6.4  
205 and 298K. Pratte and Rossi (2006) derived first-order rate constants for the reaction of  $\text{HOBr}_{(\text{aq})}$  from  
206 their uptake experiments, finding  $k^1 \sim 10^3 \text{ s}^{-1}$ .

207 The IUPAC subcommittee for gas kinetic data evaluation currently recommends an uptake  
208 coefficient parameterisation utilising accommodation coefficient  $\alpha_{\text{HOBr}} = 0.6$  (Wachsmuth et al.,  
209 2002), and first-order rate constant  $k^1 = k_{\text{ter}} \cdot [\text{H}^+_{(\text{aq})}] \cdot [\text{X}^-_{(\text{aq})}]$ , with  $k_{\text{ter}} = 2.3 \cdot 10^{10} \text{ M}^{-2} \text{ s}^{-1}$  (Liu and  
210 Margarem, 2001) for  $\text{HOBr} + \text{Cl}^-$  and  $k_{\text{ter}} = 1.6 \cdot 10^{10} \text{ M}^{-2} \text{ s}^{-1}$  (Beckwith et al., 1996) for  $\text{HOBr} + \text{Br}^-$ .  
211 Assuming a  $\text{Cl}^-_{(\text{aq})}$  concentration of 5.3 M typical of sea-water and low uptake coefficients in alkaline  
212 sea-salt aerosol (Ammann et al., 2013 and the IUPAC evaluation website), this parameterisation  
213 yields a high uptake coefficient,  $\gamma_{\text{HOBr}} \sim 0.6$ , on acidified sea-salt aerosol, and is in agreement with  
214  $\gamma_{\text{HOBr}} \geq 0.2$  reported by Abbatt and Waschewsky (1998) while overestimating the uptake coefficient  
215 as reported by Pratte and Rossi (2006) by a factor of  $\sim 20$ .

216 Here we present new uptake calculations based on the general acid assisted mechanism rather than  
217 termolecular kinetics in an attempt to consolidate these contrasting reported uptake coefficients  
218 within a single framework for the first time, and explain differences between model predictions and  
219 field observations of reactive bromine in the marine environment, as well as making first predictions  
220 of HOBr reactive uptake coefficients in volcanic plumes.

221

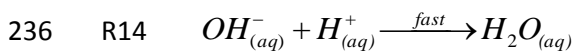
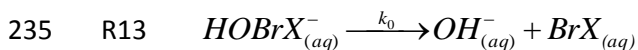
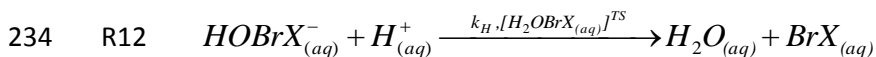
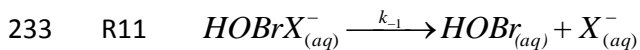
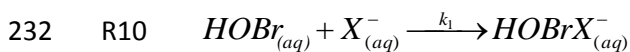
222



223 **3 Results**

224 **3.1 The second-order rate constant for aqueous-phase reaction of HOBr with halide ions**

225 In the general acid-assisted mechanism - whereby the rate of reaction of HOBr<sub>(aq)</sub> (needed in E2)  
 226 follows a second-order kinetics – an equilibrium is established between HOBrX<sup>-</sup><sub>(aq)</sub> and HOBr  
 227 according to the rate constants of R10 and R11, k<sub>1</sub> and k<sub>-1</sub> (Eigen and Kustin, 1962). The formation of  
 228 products, R12, involves a transition-state, [H<sub>2</sub>OBrX<sub>(aq)</sub>]<sup>TS</sup> that is stabilised by proton-donation to the  
 229 oxygen, with overall rate constant k<sub>H</sub>. Moreover, formation of products can also occur at low acid  
 230 concentrations via a slower pathway, R13, followed by fast reaction R14, with overall rate constant  
 231 k<sub>0</sub>.



237 According to R10-R14, the rate of reaction of HOBr<sub>(aq)</sub> can be quantified in terms of a 2<sup>nd</sup> order rate  
 238 constant (following E3 and E5) where k<sup>II</sup> is a function of pH, as described by equation E6, whose  
 239 derivation is provided in Supplementary Material.

240 E6 
$$k^{II} = \frac{k_1 \cdot (k_0 + k_H \cdot [H_{(aq)}^+])}{k_{-1} + k_0 + k_H \cdot [H_{(aq)}^+]}$$

241 In the limits of high and low acidity (E7 and E8), k<sup>II</sup> is independent of aerosol acidity. For a mid-range  
 242 acidity (k<sub>H</sub>·[H<sup>+</sup><sub>(aq)</sub>] << k<sub>-1</sub>+k<sub>0</sub>), k<sup>II</sup> becomes linearly dependent on [H<sup>+</sup><sub>(aq)</sub>] i.e. is acid-dependent (E9). In  
 243 this mid-acidity regime (only), the acid-dependence is equal to the three-body or termolecular rate  
 244 constant, k<sub>1</sub>·k<sub>H</sub>/(k<sub>-1</sub>+k<sub>0</sub>) = k<sub>ter</sub>.

245 E7  $k^{II} = k_1$  at high acidity (the limit as H<sup>+</sup><sub>(aq)</sub> tends to infinity)

246 E8  $k^{II} = \frac{k_1 \cdot k_0}{k_{-1} + k_0}$  at very low acidity (the limit as H<sup>+</sup><sub>(aq)</sub> tends to zero)

247 E9 
$$k'' = \frac{k_1 \cdot k_0}{k_{-1} + k_0} + \frac{k_1 \cdot k_H \cdot [H^+_{(aq)}]}{k_{-1} + k_0}$$

248 Equations E6-E9 describe  $k''$  in terms of four underlying rate constants ( $k_1$ ,  $k_{-1}$ ,  $k_0$ ,  $k_H$ ) and the aerosol  
 249 acidity. However, quantifying these underlying rate constants using published data is somewhat  
 250 challenging given the limited experimental data. This is now attempted below.

251

### 252 3.2 Estimating the underlying rate constants ( $k_1$ , $k_{-1}$ , $k_0$ , $k_H$ ) for HOBr+Br<sup>-</sup> and HOBr+Cl<sup>-</sup>

253 A number of aqueous-phase rate constants for the reaction of HOBr+X<sup>-</sup>+H<sup>+</sup> have been reported: For  
 254 HOBr+Br<sup>-</sup><sub>(aq)</sub>, Eigen and Kustin (1952) and Beckwith et al. (1996) report termolecular rate constants  
 255 of  $k_{\text{ter}} = 1.6 \cdot 10^{10} \text{ M}^{-2} \text{ s}^{-2}$  over a pH range of 2.7-3.6 and 1.9-2.4 at 298 K, respectively. These  
 256 experiments quantified the rate of reaction in the termolecular regime only, although Eigen and  
 257 Kustin (1962) used a consideration of relative stability constants (e.g. for equilibrium molarity of  
 258 ternary compounds X<sub>3</sub><sup>-</sup> or X<sub>2</sub>OH<sup>-</sup> relative to X<sup>-</sup>, X<sub>2</sub> or XOH) across the halogen series: HOCl+Cl<sup>-</sup>,  
 259 HOBr+Br<sup>-</sup> and HOI+I<sup>-</sup> to attempt to estimate underlying rate constants.

260 Using the reported experimental data,  $k''$  parameterisations (in terms of the underlying rate  
 261 constants ( $k_1$ ,  $k_{-1}$ ,  $k_0$  and  $k_H$ ) and acidity according to E6 derived above) are estimated as follows.

262

#### 263 3.2.1 HOBr+Br<sup>-</sup>

264 For HOBr+Br<sup>-</sup>, Eigen and Kustin (1962), proposed order of magnitude estimates of  $k_1 = 5 \cdot 10^9 \text{ M}^{-1} \text{ s}^{-1}$ ,  
 265  $k_{-1} = 5 \cdot 10^9 \text{ s}^{-1}$ ,  $k_H = 2 \cdot 10^{10} \text{ M}^{-1} \text{ s}^{-1}$ , and  $k_0 = 10^4 \text{ s}^{-1}$ . However, in Figure 4 of Beckwith et al. (1996), there  
 266 are indications of acid-saturation in their  $k''$  rate constant data for HOBr+Br<sup>-</sup>, seen as curvature in the  
 267 plots of observed  $k''$  versus acidity. This is also seen in their Figure 5 where  $k''_{\text{observed}} \geq 2.3 \cdot 10^8 \text{ M}^{-1} \text{ s}^{-1}$ .  
 268 We therefore suggest acid-saturation of the reaction between HOBr and Br<sup>-</sup> may limit  $k''$  to  $\sim 5 \cdot 10^8$   
 269  $\text{M}^{-1} \text{ s}^{-1}$ . We also adjust  $k_{-1}$  to  $k_{-1} \sim 5 \cdot 10^8 \text{ s}^{-1}$  on the basis of the reported stability constant  $k_1/k_{-1} \sim 1 \text{ M}^{-1}$   
 270 (Eigen and Kustin, 1962). While, any evidence for acid-saturation lays within the reported error bars  
 271 for the data points this adjustment does not affect our general conclusions about  $\gamma_{\text{HOBr+Br}}$  in this  
 272 study.

273

#### 274 3.2.1 HOBr+Cl<sup>-</sup>

275 For  $\text{HOBr} + \text{Cl}^-_{(\text{aq})}$ , Liu and Margareem (2001) report a three-body rate constant of  $2.3 \cdot 10^{10} \text{ M}^{-2} \text{ s}^{-2}$  in  
276 buffered aerosol at  $\text{pH} = 6.4$  and 298K. Pratte and Rossi (2006) also derived estimates for first-order  
277 rate constants for reaction of  $\text{HOBr}_{(\text{aq})}$  from their uptake coefficient experiments. We re-evaluate  
278 these data below to improve quantification of the reaction kinetics of  $\text{HOBr} + \text{Cl}^-$ .

279 For  $\text{HOBr} + \text{Cl}^-$ , the underlying rate constants ( $k_1$ ,  $k_{-1}$ ,  $k_H$ ,  $k_0$ ) are estimated as follows. The rate  
280 constant  $k_1$  is derived from the estimation of  $k^{\text{II}}$  at acid saturation (E7). For this, we estimated  $k^{\text{II}}$  at  
281  $\text{pH} -1$  to 0 from experiments of Pratte and Rossi (2006), Table 2. These new estimates of  $k^{\text{II}}$  are  
282 derived from first order  $k^{\text{I}}$  rate constants for the reaction of  $\text{HOBr}_{(\text{aq})}$ , reported by Pratte and Rossi  
283 (2006), where  $[\text{Cl}^-_{(\text{aq})}]$  is calculated by the E-AIM model from experimental conditions, E-AIM predicts  
284 chloride concentrations are reduced under the experimental conditions as consequence of acid-  
285 displacement of  $\text{HCl}_{(\text{g})}$  (see further discussion in Supplementary Material). We find  $k^{\text{II}} \sim 10^4 \text{ M}^{-1} \text{ s}^{-1}$   
286 over  $\text{pH} -1$  to 0, see Table 2 for details. We note that in their reporting of  $k^{\text{I}}$  rate constants from their  
287 uptake experiments, Pratte and Rossi, (2006) assumed an accommodation coefficient of either  $\alpha_{\text{HOBr}}$   
288  $= 0.2$  or  $\alpha_{\text{HOBr}} = 0.02$ . Given that experiments on  $\text{NaBr}_{(\text{aq})}$  aerosol have identified an accommodation  
289 coefficient for  $\text{HOBr}$  on  $\text{NaBr}_{(\text{aq})}$  particles of 0.6 (Wachsmuth et al. 2002), the  $k^{\text{II}}$  data derived  
290 assuming  $\alpha_{\text{HOBr}}=0.2$  are likely more representative. Nevertheless, either case yields estimate for  $k^{\text{II}} \sim$   
291  $10^4 \text{ M} \text{ s}^{-1}$  over  $\text{pH} = 0$  to -1. A second estimate for  $k^{\text{II}}$  is made from the reported three-body rate  
292 constant of  $2.3 \cdot 10^{10} \text{ M}^{-2} \text{ s}^{-2}$  at  $\text{pH} = 6.4$ , by setting  $k^{\text{II}} = k_{\text{ter}} \cdot [\text{H}^+_{(\text{aq})}]$ . This yields  $k^{\text{II}} = 9 \cdot 10^3 \text{ M}^{-1} \text{ s}^{-1}$  at  $\text{pH}$   
293 6.4.

294 Thus, collectively these two datasets at  $\text{pH} = 6.4$  and 0 to -1 suggest that  $k^{\text{II}}$  is acid saturated at  $\sim 10^4$   
295  $\text{M} \text{ s}^{-1}$  at  $\text{pH} \leq 6$ . Based on this value for  $k^{\text{II}}$  at acid saturation (where  $k^{\text{II}} = k_1$ ) we set  $k_1 = 1.2 \cdot 10^4 \text{ M} \text{ s}^{-1}$ ,  
296 as an average estimate, which is less than  $k_1$  for  $\text{HOBr} + \text{Br}^-$ , and which is consistent with the greater  
297 nucleophile strength of  $\text{Br}^-$  compared to  $\text{Cl}^-$ . We fix  $k_H = 2 \cdot 10^{10} \text{ M}^{-1} \text{ s}^{-1}$ , equal to that estimated by  
298 Eigen and Kustin (1961) for  $\text{HOBr} + \text{Br}^-$ , noting this reaction likely close to the diffusion limit. Our value  
299 of  $k^{\text{II}}$  for  $\text{HOBr} + \text{Cl}^-$  at low acidity ( $= (k_1 \cdot k_0) / (k_0 + k_{-1})$ ) is a similar order of magnitude to the  $k^{\text{II}}$  estimate  
300 for  $\text{HOCl} + \text{Cl}^-$  ( $\leq 0.16 \text{ M}^{-1} \text{ s}^{-1}$ , see Gerritsen and Margareem, 1989) or perhaps slightly higher (because  
301 the less electronegative Br of  $\text{HOBr}$  may be more susceptible to nucleophilic attach than  $\text{HOCl}$ ), but  
302 is substantially less than the  $k^{\text{II}}$  estimate for  $\text{HOBr} + \text{Br}^-$  ( $10^4 \text{ M}^{-1} \text{ s}^{-1}$ , Eigen and Kustin, 1962) at low  
303 acidity, and consistent with  $\text{Cl}^-$  being a weaker nucleophile than  $\text{Br}^-$ . Overall, a value for the low  
304 acidity  $k^{\text{II}}$  rate constant;  $(k_0 \cdot k_1) / (k_1 + k_{-1}) = 10^1 \text{ M}^{-1} \text{ s}^{-1}$  seems reasonable.

305 A similar analysis based on the three-body rate constant of  $2.3 \cdot 10^{10} \text{ M}^{-2} \text{ s}^{-2}$  (Liu and Magareem, 2002).  
306 yields  $k_0 = 2 \cdot 10^1 \text{ s}^{-1}$  and  $k_{-1} = 1.1 \cdot 10^4 \text{ s}^{-1}$ . These estimates for the underlying rate constants for

307 HOBr+Cl<sup>-</sup> are rather uncertain, nevertheless the most important result is the occurrence of acid-  
308 saturation of  $k^{\text{II}}$  for HOBr+Cl<sup>-</sup>, which the experimental data limits  $k^{\text{II}}$  to  $\sim 10^4 \text{ M s}^{-1}$  at  $\text{pH} \leq 6$ .

309

### 310 **3.3 A new parameterisation for the $k^{\text{II}}$ for HOBr+Br<sup>-</sup> and HOBr+Cl<sup>-</sup>**

311 The underlying rate constants ( $k_1$ ,  $k_{-1}$ ,  $k_{\text{H}}$ ,  $k_0$ ) for reaction of HOBr+Br<sup>-</sup> and HOBr+Cl<sup>-</sup> estimated above  
312 are summarized in Table 3. Our parameterisation for  $k^{\text{II}}$  based on these data, with  $k^{\text{II}}$  defined by  
313 equation E6 is shown in Figure 1 as a function of aerosol acidity, alongside the experimental values  
314 for  $k^{\text{II}}$  derived from the reported experimental data from Eigen and Kustin (1962), Beckwith et al.  
315 (1996), Liu and Margareum (2001) and Pratte and Rossi (2006) (see Table 2). As expected, the  $k^{\text{II}}$   
316 parameterisations for HOBr+Br<sup>-</sup> and HOBr+Cl<sup>-</sup> exhibit three distinct regimes:  $k^{\text{II}}$  is independent of  
317 acidity at high pH.  $k^{\text{II}}$  is dependent on acidity for a medium pH range, where the rate constant  $k^{\text{II}} =$   
318  $k_{\text{ter}} \cdot [\text{H}^+_{(\text{aq})}]$ , and in this regime the rate constant is termolecular. At high acidity,  $k^{\text{II}}$  becomes acid-  
319 independent ( $k^{\text{II}} = k_1$ ), yielding an acid-saturated  $k^{\text{II}}$  that is lower for HOBr+Cl<sup>-</sup> than HOBr+Br<sup>-</sup> given  
320 the weaker nucleophile strength.

321 Also shown in Figure 1 is the termolecular approach to HOBr kinetics assumed to date, which  
322 predicts acid-dependent  $k^{\text{II}}$  over all parameter space. Clearly, the termolecular assumption for HOBr  
323 kinetics is only valid in the termolecular regime, between pH 1-6 for HOBr+Br<sup>-</sup>, and  $> \text{pH} 6$  for  
324 HOBr+Cl<sup>-</sup>. At high acidity, the termolecular approach overestimates the rate constant compared to  
325 the  $k^{\text{II}}$  parameterisation by several orders of magnitude. The disagreement is greatest for HOBr+Cl<sup>-</sup>,  
326 where the termolecular approach overestimates the  $k^{\text{II}}$  rate constant by a factor of  $10^3$  at  $\text{pH} = 3$   
327 and  $10^6$  at  $\text{pH} = 0$ . Of interest is the effect of our revised parameterisation on the HOBr reactive  
328 uptake coefficient. Below we compare the reactive uptake coefficients of HOBr calculated our  
329 revised  $k^{\text{II}}$  parameterisation to experimental uptake coefficients reported under laboratory  
330 conditions. In section 5 we present calculations of the HOBr reactive uptake coefficient for marine  
331 and volcanic plume conditions and discuss implications for reactive halogen chemistry in these  
332 environments.

333

### 334 **3.4 Comparison of our model with experimental uptake coefficient data**

335 As discussed in the introduction, discrepancies exist in the reported reactive uptake coefficients for  
336 HOBr on acidified sea-salt aerosol. Abbatt and Waschewsky (1998) observed a strong pH  
337 dependence of the uptake onto sodium chloride aerosol, being  $1.5 \cdot 10^{-3}$  for neutral, unbuffered  
338 sodium chloride aerosol, rising to  $> 0.2$  for aerosols acidified to pH 0.3 by the addition of HCl, i.e.

339 close to the accommodation coefficient ( $\alpha = 0.6 \pm 0.2$ , Wachsmuth et al., 2002). The role of  $H^+$   
340 species in the reactive uptake process was further demonstrated by the high uptake coefficient of  $>$   
341 0.2 on aerosols buffered to pH 7 by a  $NaH_2PO_4 / Na_2HPO_4$  buffer. In contrast, Pratte and Rossi (2006)  
342 measured reactive uptake coefficients on  $H_2SO_4$ -acidified sea-salt aerosol to be  $\sim 10^{-2}$  at  $H_2SO_4:NaCl =$   
343 1.45:1, with an RH-dependence (finding  $\gamma_{HOBr} \sim 10^{-3}$  at  $RH < 70\%$ ).

344 We have calculated the reactive uptake coefficients for HOBr for the conditions of these two  
345 laboratory experiments using our new parameterisation for  $k^{\parallel}$  and the E-AIM model to determine  
346 aerosol composition.

347 Below we show that the origin for this wide discrepancy between measured HOBr uptake onto  
348 acidified bromide aerosol and chloride aerosol lies partly in the difference in reactivity of HOBr  
349 towards  $Br^-$  and  $Cl^-$ , but also in differences in aerosol composition in the two studies: HCl-acidified  
350 sea-salt aerosol retains high  $Cl^-_{(aq)}$  concentrations, whereas  $H_2SO_4$ -acidified sea-salt aerosol  
351 undergoes HCl-displacement, lowering  $Cl^-_{(aq)}$  concentrations. This acid-displacement of HCl leads to a  
352 lowering of the reactive uptake coefficient for HOBr on  $H_2SO_4$ -acidified aerosol.

353

#### 354 **3.4.1 High uptake coefficient on HCl-acidified sea-salt aerosol**

355 On HCl-acidified  $NaCl_{(aq)}$  aerosol, Abbatt and Wachowsky (1998) measured the uptake coefficient of  
356 HOBr to be  $> 0.2$ . We calculate the uptake coefficient for  $HOBr+Cl^-$  under these experimental  
357 conditions for which a chloride concentration of 6.6 M is predicted according to E-AIM (see details in  
358 Section 3.1.1 of Supplementary Material and Table 4). For particles of 1  $\mu m$  radius at 298 K, both our  
359 new parameterisation for  $k^{\parallel}$  and the termolecular approach to  $HOBr+Cl^-$  kinetics yield high uptake  
360 coefficient,  $\gamma_{HOBr+Cl^-} \sim 0.6$ , thus are consistent with the experimental findings, see Table 4.

361

#### 362 **3.4.2 Low uptake coefficient on $H_2SO_4$ -acidified sea-salt aerosol with RH dependence**

363 On  $H_2SO_4$ -acidified sea-salt aerosol, Pratte and Rossi (2006) measured the uptake coefficient of HOBr  
364 to be  $\sim 10^{-2}$  at  $H_2SO_4:NaCl = 1.45:1$ , with an RH-dependence (finding  $\gamma_{HOBr} \sim 10^{-3}$  at  $RH < 70\%$ ). Using  
365 our parameterisation, we calculate the uptake coefficient for  $HOBr+Cl^-$  under these experimental  
366 conditions, at 298 K, and with variable RH (see details in Section 3.1.2 of Supplementary Material  
367 and Table 4). We assume a solubility of HOBr in sulphuric acid of 363  $M atm^{-1}$  at 296 K (following  
368 Pratte and Rossi, 2006 based on Iraci et al. 2005), and calculate a HOBr diffusion coefficient in  
369 sulphuric acid of  $5.5 \cdot 10^{-6} cm^2 s^{-1}$  and  $1.0 \cdot 10^{-5} cm^2 s^{-1}$  at 50 and 80 % RH (48 and 29 wt%  $H_2SO_4$ )

370 respectively. E-AIM predicts the aerosol  $\text{Cl}^-_{(\text{aq})}$  concentrations to be  $0.004 \text{ M L}^{-1}$  and  $0.08 \text{ M L}^{-1}$  at 50  
371 and 80 % RH respectively, see Table 4.

372 The new parameterisation for  $k^{\text{II}}$  yields uptake coefficients for  $\text{HOBr}+\text{Cl}^-$  of  $4.4 \cdot 10^{-3}$  at 50% RH and  
373  $7.6 \cdot 10^{-2}$  at 80% RH, in broad agreement to the low uptake coefficients reported by Pratte and Rossi  
374 (2006);  $1.0 \pm 10^{-2}$  at  $\text{RH} \geq 76\%$ . Such agreement is to some extent not surprising, given the usage of  $k^{\text{I}}$   
375 reported at  $\text{RH} = 77\text{-}90\%$  from the same Pratte and Rossi (2006) experiments to derive an estimate  
376 for  $k^{\text{II}}$  at acid saturation (see Section 3 and Figure 1). Nevertheless, the uptake calculations confirm  
377 and provide a first explanation for the RH dependence of the uptake coefficient as reported by  
378 Pratte and Rossi (2006). The model indicates that the underlying cause of this trend is greater  $[\text{Cl}^-_{(\text{aq})}]$   
379 at higher RH, given higher solubility of HCl at the lower  $\text{wt}\% \text{H}_2\text{SO}_4$  at high RH. This is further shown  
380 by Figure 2 that compares the modelled and observed RH dependence of the uptake coefficient of  
381 HOBr across all reported data from 40 – 90 % RH, demonstrating broad agreement in the trend  
382 (noting discrepancies may result from impurities within the sea-salt solution or uncertainties within  
383 the parameterisations used in the uptake model). These findings are in contrast to the termolecular  
384 approach to  $k^{\text{I}}$  that yields an uptake coefficient of 0.6 at both RH values, substantially overestimating  
385  $\gamma_{\text{HOBr}}$  by at least a factor of 20 (see Table 4). This is because the termolecular approach assumes acid-  
386 dependent  $k^{\text{II}}$  across all pH, leading to an extremely high rate constant for the reaction of  $\text{HOBr}+\text{Cl}^-$   
387 at  $\text{pH} -1$  to 0, and a very fast rate of reaction of HOBr with  $\text{Cl}^-$ : even though  $\text{Cl}^-$  concentrations are  
388 depleted by acid-displacement, the assumed increased rate constant at low pH overcompensates for  
389 this effect.

390 In conclusion, our new  $k^{\text{II}}$  parameterisation for the kinetics of  $\text{HOBr}+\text{X}^-$  yields uptake coefficients in  
391 agreement with reported laboratory data, and -for the first time- reconciles differences between  
392 reported uptake on HCl-acidified and  $\text{H}_2\text{SO}_4$ -acidified sea-salt aerosols, within a single framework.

393

#### 394 **4 Implications for BrO chemistry in the marine and volcanic environments**

##### 395 **4.1 Declining uptake coefficients on progressively $\text{H}_2\text{SO}_4$ -acidified sea-salt aerosol**

396 Using the revised HOBr reaction kinetics (Figure 1), the  $\text{HOBr}+\text{Br}^-$  and  $\text{HOBr}+\text{Cl}^-$  reactive uptake  
397 coefficients are now re-evaluated for a model sea-salt aerosol that undergoes progressive  $\text{H}_2\text{SO}_4$ -  
398 acidification (Figure 3) and compared to calculations using the termolecular approach. We  
399 investigate how the reductions in halide ion concentrations caused by the  $\text{H}_2\text{SO}_{4(\text{aq})}$  addition (through  
400 both acid-displacement reactions that deplete  $[\text{Cl}^-_{(\text{aq})}]$ , and dilution of  $[\text{Br}^-_{(\text{aq})}]$  by  $\text{H}_2\text{SO}_{4(\text{aq})}$  volume)  
401 impact  $\gamma_{\text{HOBr}}$  at low pH.

402 A particle radius of 1 or 0.1  $\mu\text{m}$  is assumed in the uptake calculation. Temperature is set to 298 K and  
403  $\text{RH} = 80\%$  (above deliquescence). For aerosol that is alkaline or only weakly acidic (pH 12 to pH 4),  
404 uptake coefficients were calculated assuming a fixed sea-salt composition with  $[\text{Cl}^-_{(\text{aq})}] = 5.3 \text{ Mol L}^{-1}$   
405 and  $[\text{Br}^-_{(\text{aq})}] = 0.008 \text{ Mol L}^{-1}$ , with pH varied between 4 and 12 (E-AIM was not used given very low  
406 degree of  $\text{H}_2\text{SO}_4$ -acidification). For more strongly acidified sea-salt, across  $\text{H}_2\text{SO}_4:\text{Na}$  ratios from 0.05  
407 to 400 (pH 4 to -0.87 for the model aerosol conditions), E-AIM was used to determine the extent of  
408 acid-displacement of HCl from acidified  $\text{NaCl}_{(\text{aq})}$  aerosol, with aerosol  $\text{Br}_{(\text{aq})}^-$  determined using an  
409 effective Henry's law solubility for HBr (see predicted composition in Supp. Material Section 3.2).

410 Figure 4 shows the calculated reactive uptake for  $\text{HOBr}+\text{Br}^-$  and  $\text{HOBr}+\text{Cl}^-$  increase with increasing  
411 acidity over pH 4-12 for the uptake coefficient for 0.1 and 1  $\mu\text{m}$  radius particles, similar to that  
412 previously reported using the termolecular approach. The alkaline to acid transition in  $\gamma_{\text{HOBr}}$  reflects  
413 the increase in the underlying  $\text{HOBr}_{(\text{aq})}$   $k^{\text{I}}$  rate constant with acidity due to the onset of the acid  
414 assisted mechanism, Figure 1 as well as the decrease of HOBr partitioning to  $\text{BrO}^-$ .  $\gamma_{\text{HOBr}+\text{Cl}^-}$  reaches  
415 values close to the accommodation limit by  $\text{pH} \leq 8$  (for 1  $\mu\text{m}$  radius particles) or  $\text{pH} \leq 7$  (for 0.1  $\mu\text{m}$   
416 radius particles) while  $\gamma_{\text{HOBr}+\text{Br}^-}$  reaches values close to the accommodation limit by  $\text{pH} \leq 5$  (for 1  $\mu\text{m}$   
417 radius particles) or  $\text{pH} \leq 4$  (for 0.1  $\mu\text{m}$  radius particles).

418 In the high acidity regime, the acid-saturation of  $k^{\text{II}}$  can cause  $\gamma_{\text{HOBr}}$  to plateau at a level slightly lower  
419 than  $\alpha_{\text{HOBr}}$  (e.g. in  $\gamma_{\text{HOBr}+\text{Cl}^-}$  at  $\text{pH} \sim 4$ ), in contrast to the termolecular approach. Overall, for slightly-  
420 acidified sea-salt aerosol, reactive uptake of HOBr is driven primarily by  $\gamma_{\text{HOBr}+\text{Cl}^-}$ .  $\gamma_{\text{HOBr}+\text{Br}^-}$  reaches  
421 similar values to  $\gamma_{\text{HOBr}+\text{Cl}^-}$  at  $\text{pH} \sim 3-4$  for the specific model aerosol conditions of this study.

422 However, as the degree acidification by  $\text{H}_2\text{SO}_4$  increases, the uptake coefficient for  $\text{HOBr}+\text{Cl}^-$  begins  
423 to decline at  $\text{pH} < 4$ . This is due to acid-displacement reactions that convert  $\text{Cl}^-_{(\text{aq})}$  into  $\text{HCl}_{(\text{g})}$ , thereby  
424 lowering  $[\text{Cl}^-_{(\text{aq})}]$ . This leads to  $\gamma_{\text{HOBr}+\text{Cl}^-} < \gamma_{\text{HOBr}+\text{Br}^-}$ , i.e. HOBr reactive uptake becomes driven by  
425  $\text{HOBr}+\text{Br}^-$  below a pH of  $\sim 2$  for the specific aerosol conditions of this study. As  $\text{H}_2\text{SO}_4:\text{Na}$  ratio  
426 increases further and pH decreases further, the uptake coefficient for  $\text{HOBr}+\text{Br}^-_{(\text{aq})}$  also begins to  
427 decline. This is principally due to the dilution of  $\text{Br}^-_{(\text{aq})}$  by the additional volume of  $\text{H}_2\text{SO}_{4(\text{aq})}$  that  
428 becomes important particularly at very high  $\text{H}_2\text{SO}_4:\text{Na}$  (see E-AIM calculations in Supplementary  
429 Materials).

430 Notably, the declines in uptake coefficients are greatest for smaller particles, for which there is a  
431 greater probability that  $\text{HOBr}_{(\text{aq})}$  may diffuse across the particle and be released to the gas phase,  
432 without any aqueous-phase reaction occurring.

433 The uptake coefficients are also further reduced if parameterisations for the solubility of HOBr in  
434  $\text{H}_2\text{SO}_{4(\text{aq})}$  is assumed in the uptake equation rather than that for water. The exact point of transition  
435 between these two parameterisations is not well constrained, but it is clear that the  $\text{H}_2\text{SO}_{4(\text{aq})}$   
436 parameterisations become more applicable than water with greater acidification, and must certainly  
437 be more relevant at high  $\text{H}_2\text{SO}_4\text{:Na}$ . The lower solubility of HOBr in  $\text{H}_2\text{SO}_{4(\text{aq})}$  acts to decrease the  
438 uptake coefficient, and is found to have a stronger impact on  $\gamma_{\text{HOBr}}$  than the slower rate of diffusion  
439 of  $\text{HOBr}_{(\text{aq})}$  in  $\text{H}_2\text{SO}_4$ .

440 In summary, following a rise over the alkaline-acid transition, our revised HOBr kinetics yields HOBr  
441 reactive uptake coefficients that subsequently decline on progressively  $\text{H}_2\text{SO}_4$ -acidified sea-salt  
442 aerosol. For the aerosol concentration assumed, the uptake coefficient on the  $0.1 \mu\text{m}$  radius  
443 particles declines to  $\gamma_{\text{HOBr}+\text{Br}} < 0.03$  at a  $\text{H}_2\text{SO}_4\text{:Na}$  ratio of 400:1, indicating that the reactive uptake of  
444 HOBr on highly acidified sub-micrometer particles is extremely low, Figure 3. These decreases in  
445 uptake coefficient with increasing aerosol acidity are not captured by calculations that assume  
446 termolecular kinetics. As stated in the previous section, this is because the termolecular approach  
447 assumes the HOBr rate constant is acid-dependent across all pH, and does not consider acid-  
448 saturation of the rate constant.

449

#### 450 **4.2 Implications for BrO chemistry in the marine boundary layer**

451 Figure 4 shows clearly that higher acidity does not necessarily lead to faster production of reactive  
452 bromine. It is well-known that acidity is required for reactive bromine formation to occur:  $\text{H}^+_{(\text{aq})}$  is  
453 consumed in the reaction, therefore a source of acidity is required to sustain prolonged BrO  
454 formation chemistry. Further, under alkaline conditions HOBr dissociates into less reactive OBr<sup>-</sup>.  
455 However, the  $\gamma_{\text{HOBr}}$  dependency on acidity shown here suggests that additional aerosol acidification  
456 by  $\text{H}_2\text{SO}_{4(\text{aq})}$  can act as a limitation to the formation of reactive bromine via HOBr uptake, particularly  
457 for small particle sizes.

458 This leads to the following implications for BrO chemistry in the marine environment, where both  
459 supra-micron and sub-micron particles are reported, the former typically being moderately acidified  
460 perhaps with some Cl<sup>-</sup>-depletion, and the latter being dominated by  $\text{H}_2\text{SO}_4$  with only a trace quantity  
461 of sea-salt (e.g. Keene et al., 2002):

462 Firstly, the reactive uptake of HOBr is driven by reaction with  $\text{Br}^-$  as  $\gamma_{\text{HOBr}+\text{Cl}}$  is reduced on  $\text{H}_2\text{SO}_4$ -  
463 acidified (Cl<sup>-</sup>-depleted) sea-salt aerosol. This leads to a negative feedback in the uptake coefficient  
464 for HOBr with BrO chemistry evolution over time, as the conversion of  $\text{Br}^-_{(\text{aq})}$  to  $\text{Br}_{2(\text{g})}$  acts to decrease



465 aerosol [ $\text{Br}^-_{(\text{aq})}$ ], reducing subsequent values of  $\gamma_{\text{HOBr}+\text{Br}^-}$ . This negative feedback for  $\gamma_{\text{HOBr}+\text{Br}^-}$  will play a  
466 much more significant role for overall HOBr reactive uptake according our revised HOBr kinetics than  
467 has been assumed by model studies to date based on the termolecular approach (for which  $\gamma_{\text{HOBr}+\text{Cl}^-} \geq$   
468  $\gamma_{\text{HOBr}+\text{Br}^-}$ ).

469 Secondly, very low reactive uptake coefficients for both HOBr+Br<sup>-</sup> and HOBr+Cl<sup>-</sup> are predicted for  
470 sub-micron particles at high H<sub>2</sub>SO<sub>4</sub>:Na ratios (e.g.  $\gamma_{\text{HOBr}} < 0.03$ , see Figure 4). Such low  $\gamma_{\text{HOBr}}$  is  
471 proposed as a first explanation for the absence of observable  $\text{Br}^-_{(\text{aq})}$  depletion in sub-micron H<sub>2</sub>SO<sub>4</sub><sup>-</sup>  
472 dominated particles in the marine environment, in contrast to supra-micron particles where  $\text{Br}^-_{(\text{aq})}$   
473 depletion is observed and interpreted as evidence of HOBr reactive uptake to form reactive bromine  
474 (Sander et al., 2003). Indeed, observations find the submicron H<sub>2</sub>SO<sub>4</sub>-dominated aerosol to be  
475 enriched in  $\text{Br}^-_{(\text{aq})}$  relative to expected concentrations based on the particle Na<sup>+</sup> content (Sander et  
476 al., 2003). A plausible explanation is that the release of  $\text{Br}_{2(\text{g})}$  from the supra-micron particles leads to  
477 the continual formation of gas-phase reactive bromine species of which a proportion will ultimately  
478 be deposited back to (both types of) marine aerosols as a source of  $\text{Br}^-_{(\text{aq})}$ . The net effect is for  $\text{Br}^-_{(\text{aq})}$   
479 concentrations to become enhanced (relative to Na) in the sub-micron aerosol where  $\gamma_{\text{HOBr}}$  is low  
480 simultaneous to becoming depleted in the supra-micron aerosol where  $\gamma_{\text{HOBr}}$  is high. For the former,  
481 an upper limit must exist to the extent Br-enrichment can occur whilst maintaining the relatively low  
482  $\gamma_{\text{HOBr}+\text{Br}^-}$ . Importantly, this argumentation is only possible using our new uptake calculations based on  
483  $k^{\text{I}}$  calculated using revised HOBr kinetics in terms of  $k^{\text{II}}$ , as the termolecular approach predicts high  
484 HOBr reactive uptake for both particle types. We encourage our new rate constants calculations for  
485 HOBr reactive uptake to be incorporated into numerical models to test and quantify potential  
486 submicron aerosol Br<sup>-</sup> enrichment via this proposed mechanism.

487 We further suggest both of the abovementioned factors may also contribute underlying reasons for  
488 the reported over-prediction by numerical models of BrO cycling in the marine environment (Sander  
489 et al., 2003; Smoydzin and von Glasow, 2007; Keene et al., 2009). Inclusion of the new HOBr kinetics  
490 into such models will allow this hypothesis to be tested and quantified.

491

#### 492 **4.3 Reactive uptake of HOBr on volcanic aerosol**

493 HOBr reactive uptake coefficients are now calculated for the first time onto aerosol in a halogen-rich  
494 volcano plume, using the  $k^{\text{II}}$  parameterisations for HOBr+Br<sup>-</sup> and HOBr+Cl<sup>-</sup>. Using the volcanic aerosol  
495 composition predicted by E-AIM (based on Etna emission scenario, see section 3.3 of Supplementary  
496 Material), uptake coefficients for HOBr+Br<sup>-</sup> and HOBr+Cl<sup>-</sup> are calculated across tropospheric

497 temperature and relative humidity, for two plume dilutions (30 and 0.3  $\mu\text{mol}/\text{m}^3$ , which are  
498 equivalent to  $\sim 1$  ppmv, and 0.01 ppmv  $\text{SO}_2$  at 4 km altitude in US standard atmosphere), and  
499 assuming a particle radius of 1  $\mu\text{m}$ , Figure 4. There exists no experimental information regarding the  
500 temperature dependence of  $k^{\text{II}}$  for  $\text{HOBr}+\text{X}$ . Here it is assumed the variation  $k^{\text{II}}$  with temperature  
501 over 230-300 K is small compared to the temperature dependence of the  $\text{HOBr}$  and  $\text{HX}$  solubilities  
502 (which vary by several orders of magnitude over the parameter space).

503 High  $\text{HOBr}$  uptake coefficients are predicted at low tropospheric temperatures:  $\gamma_{\text{HOBr}+\text{Br}^-} \approx \gamma_{\text{HOBr}+\text{Cl}^-} \approx$   
504 0.6. The uptake coefficient decreases markedly with increasing temperature for  $\gamma_{\text{HOBr}+\text{Cl}^-}$  and also  
505 decreases for  $\gamma_{\text{HOBr}+\text{Br}^-}$  in the most dilute plume scenario. The inverse temperature trend in  $\gamma_{\text{HOBr}}$  is  
506 caused by a lower solubility of  $\text{HX}$  in sulphuric acid particles at higher tropospheric temperatures  
507 (particularly for  $\text{HCl}$ ), augmented by a similar temperature trend in the solubility of  $\text{HOBr}_{(\text{aq})}$ . The  
508 variation with plume dilution is explained by the fact that lower gas-to-aerosol partitioning yields  
509 lower  $[\text{X}^-_{(\text{aq})}]$  in the dilute plume scenarios thus a lower  $k^{\text{I}} = k^{\text{II}} \cdot [\text{X}^-_{(\text{aq})}]$  in the uptake equation, hence a  
510 reduced  $\gamma_{\text{HOBr}}$ . Figure 4 also illustrates a weak dependence of the uptake coefficients on relative  
511 humidity. This is due to increasing solubility of the halides with  $\text{RH}$  or lower  $\text{wt}\% \text{H}_2\text{SO}_4$  (potential  $\text{RH}$ -  
512 dependence of  $\text{HOBr}$  solubility is not considered in the parameterisations, see Supplementary  
513 Material). As for the marine aerosol study, reductions in  $\gamma_{\text{HOBr}}$  are more pronounced for particles of  
514 smaller radii (data not shown), as the probability for diffusion across the particle without reaction is  
515 higher. According to Figure 4,  $\gamma_{\text{HOBr}+\text{Br}^-}$  is equal to or exceeds  $\gamma_{\text{HOBr}+\text{Cl}^-}$  under all temperature and  
516 humidity scenarios for the composition of the Etna emission. This is driven by higher  $k^{\text{I}}$  in the uptake  
517 calculation (where  $k^{\text{I}} = k^{\text{II}} \cdot [\text{X}^-]$  with  $k^{\text{II}}$  a function of  $\text{pH}$ ), due to the greater saturation value  $k^{\text{II}}$  for  
518  $\text{HOBr}+\text{Br}^-$  at high acidity, and the higher solubility of  $\text{HBr}$  compared to  $\text{HCl}$ . Again it is important to  
519 note that this uptake re-evaluation using revised  $\text{HOBr}$  kinetics differs from that calculated using the  
520 termolecular approach (also shown in Figure 4) which yields high and typically accommodation  
521 limited  $\text{HOBr}$  uptake coefficients throughout the parameter space. Indeed, this is due to the fact that  
522 with the termolecular approach ( $k^{\text{I}} = k_{\text{ter}} \cdot [\text{H}^+_{(\text{aq})}] \cdot [\text{X}^-_{(\text{aq})}]$ ) the increased value of  $k_{\text{ter}}$  at high acidity more  
523 than compensates for the acidity-driven decreases in  $\text{X}^-$ , thus yielding high  $k^{\text{I}}$  and high  $\gamma_{\text{HOBr}}$ .

524

525 Figure 4 shows that in concentrated plumes near to the volcanic source, the aqueous-phase halide  
526 concentrations are sufficiently high that  $\gamma_{\text{HOBr}+\text{Br}^-}$  is accommodation-limited. Rapid formation of  $\text{BrO}$  is  
527 expected to occur. This is consistent with observations of volcanic  $\text{BrO}$  at numerous volcanoes  
528 globally (e.g. Bobrowski et al., 2007b, Boichu et al., 2011, and references therein), including  
529 emissions from both low and high altitude volcanoes, explosive eruptions and from passive

530 degassing. However, it is anticipated that the reactive uptake coefficient for HOBr+Br<sup>-</sup> will be  
531 reduced as BrO chemistry progresses causing Br<sup>-</sup><sub>(aq)</sub> concentrations to decline (due to conversion of  
532 HBr into reactive bromine). This will likely slow the BrO cycling in the more evolved plume. Plumes  
533 will also become more dilute over time due to dispersion. Figure 4 predicts this will lead to a  
534 reduction in the HOBr reactive uptake coefficient particularly in plumes confined to the lower  
535 troposphere, which may contribute to a slower rate of BrO cycling. For plumes in the mid-upper  
536 troposphere,  $\gamma_{\text{HOBr}}$  is predicted to remain high.

537 To date, numerical model studies of the impacts of volcanic halogens reactive halogen chemistry in  
538 the troposphere have either used a fixed uptake coefficient (Roberts et al., 2009; 2014, Kelly et al.,  
539 2013) or the termolecular approach to HOBr kinetics (Bobrowski et al., 2009; von Glasow, 2010).  
540 Figure 4 illustrates both of these approaches will lead to modelling inaccuracies, particularly in the  
541 downwind plume. Incorporation of more realistic HOBr kinetics in these models, using the  
542 parameterisations proposed here, is recommended in order to accurately simulate the reactive  
543 bromine chemistry and plume impacts.

544

## 545 **5 Conclusions**

546 This study introduces a new evaluation of HOBr reactive uptake coefficients on aerosol of different  
547 compositions, in the context of the general acid assisted mechanism. We emphasise that the  
548 termolecular kinetic approach assumed in numerical model studies of tropospheric reactive bromine  
549 chemistry to date is strictly only valid for a specific pH range. Rather, according to the general acid  
550 assisted mechanism, the reaction kinetics for HOBr becomes independent of pH at high acidity. By  
551 re-evaluation of reported rate constant data from uptake experiments on acidified sea-salt aerosol,  
552 and consideration of relative reaction rates according to nucleophile strength, we identify the  
553 kinetics of HOBr+Cl<sup>-</sup> may saturate below pH 6 to yield a second-order rate constant of  $k^{\text{II}} \sim 10^4 \text{ M s}^{-1}$ .  
554 The kinetics of HOBr+Br<sup>-</sup> saturates at  $k^{\text{II}} \sim 10^8\text{-}10^9 \text{ M s}^{-1}$  at pH < ~1 based on experimental data and  
555 kinetics estimates of Eigen and Kustin (1962) and Beckwith et al. (1996).

556 This study reconciles for the first time the different reported uptake reactive coefficient from  
557 laboratory experiments. The new  $k^{\text{II}}$  parameterisation yields uptake coefficients that are consistent  
558 with reported uptake experiments:  $\gamma_{\text{HOBr}} = 0.6$  on super-saturated NaBr aerosol (Wachsmuth et  
559 al.2002);  $\gamma_{\text{HOBr}} > 0.2$  on HCl-acidified sea-salt aerosol (Abbatt and Wachsewsky 1998),  $\gamma_{\text{HOBr}} = 10^{-2}$  on  
560 H<sub>2</sub>SO<sub>4</sub>-acidified sea-salt aerosol, with an RH dependence (Pratte and Rossi, 2006). The variation in  
561 uptake coefficient across the alkaline-aerosol transition is similar to that previously predicted using

562 the termolecular approach but uptake calculations using our revised kinetics of HOBr show much  
563 lower uptake coefficients for HOBr in highly acidified sea-salt aerosol, particularly for small particle  
564 radii. This is due to acid-displacement of  $\text{HCl}_{(g)}$  at high acidity slowing the rate of reaction of  $\text{HOBr}+\text{Cl}^-$   
565 , thus lowering  $\gamma_{\text{HOBr}+\text{Cl}^-}$ , with dilution of  $[\text{Br}^-_{(aq)}]$  at very high  $\text{H}_2\text{SO}_4$ :sea-salt ratios slowing the rate of  
566 reaction of  $\text{HOBr}+\text{Br}^-$ , thus lowering  $\gamma_{\text{HOBr}+\text{Br}^-}$ . This finding contrasts to the existing termolecular  
567 approach to uptake calculations in which the higher rate constant overcompensates for the decrease  
568 in halide concentration with increasing acidity. Thus, the termolecular approach, as currently used in  
569 numerical models of tropospheric BrO chemistry, may cause HOBr reactive uptake to be  
570 substantially over estimated in aerosol at high acidity.

571 Implications for BrO chemistry in the marine boundary layer have been discussed. Firstly, the HOBr  
572 uptake coefficient is predicted to be high on slightly acidified supra-micron particles but extremely  
573 low on highly-acidified sub-micron particles. A first explanation for the observed Br-enrichment in  
574 the sub-micron particles simultaneous to Br-depletion in supra-micron particles is thereby proposed,  
575 as reactive bromine release from the supra-micron fraction may deposit and accumulate in the  
576 submicron fraction, that does not undergo significant Br- depletion. Secondly, because the  $\text{HOBr}+\text{Br}^-$   
577 uptake coefficient is a function of  $\text{Br}^-_{(aq)}$  concentrations, a negative feedback can occur as the marine  
578 BrO chemistry evolves, and supramicron particle  $\text{Br}^-_{(aq)}$  concentrations are lowered by the release of  
579 reactive bromine. According to our revised HOBr kinetics (yielding  $\gamma_{\text{HOBr}+\text{Br}^-} > \gamma_{\text{HOBr}+\text{Cl}^-}$ ), this negative  
580 feedback for  $\gamma_{\text{HOBr}+\text{Br}^-}$  exerts a stronger overall influence on the rate of HOBr reactive uptake than  
581 previous studies have assumed.

582 Calculations on volcanic aerosol show that uptake is high and accommodation limited in the  
583 concentrated near-source plume, enabling BrO formation to rapidly occur. Uptake coefficients are  
584 reduced in more dilute plumes, particularly for  $\text{HOBr}+\text{Cl}^-$ , at high temperatures (typical lower  
585 tropospheric altitudes), for small particle radii. The findings suggest that HOBr uptake on sulphate  
586 aerosol directly emitted from volcanoes can readily promote BrO cycling in plumes throughout the  
587 troposphere but that the rate of BrO cycling may be reduced by low uptake coefficients in the  
588 dispersed downwind plume, particularly at lower tropospheric altitudes. Inclusion of our revised  
589 HOBr reaction kinetics in numerical models of volcanic plume chemistry (or uptake coefficients  
590 derived therefrom) is required to accurately predict the impacts of volcanic halogens on the  
591 troposphere.

592

593 **Acknowledgements**

594 TJR and LJ are grateful for funding from LABEX VOLTAIRE (VOLatils- Terre Atmosphère Interactions -  
595 Ressources et Environnement) ANR-10-LABX-100-01 (2011-20). PTG acknowledges the ERC for  
596 funding.  
597

598 **References**

- 599 Abbatt J. P. D. and Waschewsky G. C.G.: Heterogeneous Interactions of HOBr, HNO<sub>3</sub>, O<sub>3</sub>, and NO<sub>2</sub>  
600 with Deliquescent NaCl Aerosols at Room Temperature, *J. Phys. Chem. A*, 102, 3719-3725, 1998.
- 601 Ammann, M., Cox, R. A., Crowley, J.N., Jenkin, M. E., Mellouki, A., Rossi, M. J., Troe, J., and  
602 Wallington, T. J.: Evaluated kinetic and photochemical data for atmospheric chemistry: Volume VI –  
603 heterogeneous reactions with liquid substrates, *Atmos. Chem. Phys.*, 13, 8045 - 8228, 2013.
- 604 Barrie L. A., Bottenheim J. W., Schnell R. C., Crutzen P. J., Rasmussen R. A.: Ozone destruction and  
605 photochemical reactions at polar sunrise in the lower Arctic atmosphere, *Nature*, 334, 138-141,  
606 1998.
- 607 Beckwith R. C., Wang T. X., and Margerum D. W.: Equilibrium and Kinetics of Bromine Hydrolysis,  
608 *Inorg. Chem.*, 35, 995-1000, 1996.
- 609 Blatchley, E. R., R. W. Johnson, J. E. Alleman and W. F. McCoy : Effective Henry's law constants for  
610 free chlorine and free bromine, *Water Research*, 26, 99-106, 1991.
- 611 Bobrowski, N., Honniger, G., Galle, B. and Platt, U.: Detection of bromine monoxide in a volcanic  
612 plume. *Nature*, 423, 273-276, doi:10.1038/nature01625, 2003.
- 613 Bobrowski, N., von Glasow, R., Aiuppa, A., Inguaggiato, S., Louban, I., Ibrahim, O. W. and Platt, U.:  
614 Reactive halogen chemistry in volcanic plumes, *J. Geophys. Res.*, 112, D06311,  
615 doi:101029/2006JD007206, 2007a.
- 616 Bobrowski, N. and Platt, U.: SO<sub>2</sub>/BrO ratios studied in five volcanic plumes. *J. Volcanol. Geoth. Res.*,  
617 166, 3-4, 147-160, 10.1016/j.jvolgeores.2007.07.003, 2007b.
- 618 Boichu, M., Oppenheimer C., Roberts T. J., Tsanev V., Kyle P. R.: On bromine, nitrogen oxides and  
619 ozone depletion in the tropospheric plume of Erebus volcano (Antarctica), *Atmos. Environ.*, 45, 23,  
620 3856-3866, 2011.
- 621 Breider T. J., Chipperfield M. P., Richards N. A. D., Carslaw K. S., Mann G. W., Spracklen D. V.: Impact  
622 of BrO on dimethylsulfide in the remote marine boundary layer, *Geophys. Res. Lett.*, 37, L02807,  
623 doi:10.1029/2009GL040868., 2010.
- 624 Carslaw K. S., Clegg S. L. and Brimblecombe P.: A thermodynamic model of the system HCl - HNO<sub>3</sub> -  
625 H<sub>2</sub>SO<sub>4</sub> - H<sub>2</sub>O, including solubilities of HBr, from <200 K to 328 K. *J. Phys. Chem.* 99, 11557-11574,  
626 1995.

627 Clegg S. L., Brimblecombe P. and Wexler A. S., A thermodynamic model of the system  $H^+$  -  $NH_4^+$  -  $Na^+$   
628 -  $SO_4^{2-}$  -  $NO_3^-$  -  $Cl^-$  -  $H_2O$  at 298.15 K. *J. Phys. Chem. A* 102, 2155-2171, 1998.

629 Eigen M. and Kustin K.: The Kinetics of Halogen Hydrolysis, *J. Am. Chem. Soc.*, 1962, 84 (8), pp 1355–  
630 1361, DOI: 10.1021/ja00867a005, 1962.

631 Fickert S., Adams J. W. and Crowley J. N.: Activation of  $Br_2$  and  $BrCl$  via uptake of  $HOBr$  onto aqueous  
632 salt solutions, *Journal of Geophysical Research*, 104, D19, 23719-23727, 1999.

633 Frenzel A., Scheer V., Sikorski R., George Ch., Behnke W., and Zetzsch C.: Heterogeneous  
634 Interconversion Reactions of  $BrNO_2$ ,  $ClNO_2$ ,  $Br_2$ , and  $Cl_2$ ., *J. Phys. Chem. A*, 102, 1329-1337, 1998.

635 Gerritsen C.M. and Margareem D. W.: Non-Metal Redox Kinetics: Hypochlorite and Hypochlorous Acid  
636 Reactions with Cyanide, *Inorg. Chem.*, 29, 2757-2762, 1990.

637 Iraci L. T., Michelsen R. R., Ashbourn S. F. M., Rammer T. A., and Golden D. M.: Uptake of  
638 hypobromous acid ( $HOBr$ ) by aqueous sulfuric acid solutions: low-temperature solubility and  
639 reaction, *Atmos. Chem. Phys.*, 5, 1577–1587, 2005.

640 IUPAC Task Group on Atmospheric Chemical Kinetic Data Evaluation, <http://iupac.pole-ether.fr>.

641 Liu Q. and Margareem D. W.: Equilibrium and Kinetics of Bromine, *Environ. Sci. Technol.*, 35, 1127-  
642 1133, 2001.

643 Keene W.C., Pszenny A.A.P., Maben J.R., and Sander R.: Variation of marine aerosol acidity with  
644 particle size, *Geophysical research Letters*, 29, 7, 1101, 10.1029/2001GL013881, 2002.

645 Keene W. C., Long M. S., Pszenny A. A. P. Sander R., Maben J. R., Wall A. J., O'Halloran T. L., Kerkweg  
646 A., Fischer E. V., and Schrem O.: Latitudinal variation in the multiphase chemical processing of  
647 inorganic halogens and related species over the eastern North and South Atlantic Oceans, *Atmos.*  
648 *Chem. Phys.*, 9, 7361–7385, 2009.

649 Kelly P J., Kern C., Roberts T. J., Lopez T., Werner C., Aiuppa A., Rapid chemical evolution of  
650 tropospheric volcanic emissions from Redoubt Volcano, Alaska, based on observations of ozone and  
651 halogen-containing gases, *Journal of Volcanology and Geothermal Research*, Volume 259, Pages 317-  
652 333, 2013.

653 Klassen, J. K., Hu, Z. and Williams, L. R.: Diffusion coefficients for  $HCl$  and  $HBr$  in 30 wt % to 72 wt %  
654 sulfuric acid at temperatures between 220 and 300 K, *J. Geophys. Res.* 103, 16197-16202, 1998.

655 Kumar K. and Margareem D. W.: Kinetics and Mechanism of General- Acid-Assisted Oxidation of  
656 Bromide by Hypochlorite and Hypochlorous Acid, *Inorg. Chem.* 26, 2706-2711,1987.

657 Martin R.S.,<sup>2</sup> Wheeler J.C., Ilyinskaya E., Braban C.F. and Oppenheimer C: The uptake of halogen  
658 (HF, HCl, HBr and HI) and nitric (HNO<sub>3</sub>) acids into acidic sulphate particles in quiescent volcanic  
659 plumes, *Chemical Geology* 296-297, 19–25, 2012.

660 Nagy J.C., Kumar K., Margareem D. W.: Non-Metal Redox Kinetics: Oxidation of Iodide by  
661 Hypochlorous Acid and by Nitrogen Trichloride Measured by the Pulsed-Accelerated-Flow Method,  
662 *Inorganic Chemistry*, Vol. 27, No. 16, 2773-2780, 1988.

663 Nagy P. and Ashby M.T.: Reactive Sulfur Species: Kinetics and Mechanisms of the Oxidation of  
664 Cysteine by Hypohalous Acid to Give Cysteine Sulfenic Acid, *J. Am Chem Soc*, 129, 14082-14091,  
665 2007.

666 Parrella J. P., Jacob D. J., Liang Q., Zhang Y., Mickley L. J., Miller B., Evans, M. J., Yang X., Pyle J. A.,  
667 Theys N., and Van Roozendaal M.: Tropospheric bromine chemistry: implications for present and  
668 pre-industrial ozone and mercury, *Atmos. Chem. Phys.*, 12, 6723-6740, 2012.

669 Pratte P. and Rossi M. J.: The heterogeneous kinetics of HOBr and HOCl on acidified sea salt and  
670 model aerosol at 40–90% relative humidity and ambient temperature, *Physical Chemistry Chemical*  
671 *Physics*, 8, 3988–4001, 2006.

672 Read K. A., Mahajan A. S., Carpenter L. J., Evans M. J., Faria B. V. E., Heard D. E., Hopkins J. R., Lee L.  
673 D., Moller S. J., Lewis A. C., Mendes L., McQuaid J. B., Oetjen H., Saiz-Lopez A., Pilling M. J. and Plane  
674 J. M. C., Extensive halogen-mediated ozone destruction over the tropical Atlantic Ocean, *Nature*,  
675 453, doi:10.1038/nature07035, 1232-1235, 2008.

676 Roberts, T. J., Braban, C. F., Martin, R. S., Oppenheimer, C., Adams, J. W., Cox, R. A., Jones R. L. and  
677 Griffiths., P. T, Modelling reactive halogen formation and ozone depletion in volcanic plumes. *Chem.*  
678 *Geol.*, 263,151-163, 2009.

679 Roberts T.J., Martin R.S, Jourdain L.,: Reactive halogen chemistry in Mt Etna’s volcanic plume: the  
680 influence of total Br, high temperature processing, aerosol loading and plume dispersion, *ACPD*,  
681 2014.

682 Saiz-Lopez A., and von Glasow R., Reactive halogen chemistry in the troposphere, *Chem Soc Rev*,  
683 41,6448-6472, 2012.

684 Sander R., Keen W. C., Pszenny A. A. P., Arimoto R., Ayers G. P., Baboukas E., Caine J. M., Crutzen P.  
685 J., Duce R. A., Hönninger G., Huebert B. J., Maenhaut W., Mihalopoulos N., Turekian V. C., and Van  
686 Dingenen R.: Inorganic bromine in the marine boundary layer: a critical review, *Atmos. Chem. Phys.*,  
687 3, 1301-1336, 2003.



688 Sander R., Baumgaertner A., Gromov S., Harder H., Jöckel P., Kerkweg A., Kubistan D., Regelin E.,  
689 Riede H., Sandu A., Taraborelli D., Tost H. and Xie Z.-Q.: The atmospheric chemistry box model  
690 CAABA/MECCA-3.0, *Geosci. Model Dev.*, 4, 373–380, 2011.

691 Sander R., *Compilation of Henry's Law Constants for Inorganic and Organic Species of Potential*  
692 *Importance in Environmental Chemistry (Version 3)*, <http://www.henrys-law.org> accessed November  
693 2013, 1999.

694 Schmodzin L. and von Glasow R.: Do organic surface films on sea salt aerosols influence atmospheric  
695 chemistry? – a model study, *Atmos. Chem. Phys.*, 7, 5555-5567, doi:10.5194/acp-7-5555-2007, 2007.

696 Schroeder W.H., Anlauf K. G., Barrie L. A., Lu J. Y., Steffen A., Schneeberger D. R. and Berg T.: Arctic  
697 springtime depletion of mercury, *Nature*, 394, 331-332, doi:10.1038/28530, 1998.

698 Schweizer F., Mirabel P. and George C., Uptake of hydrogen halides by water droplets, *J. Phys Chem*  
699 *A.*, 104, 72-76, 2000.

700 Seinfeld, John H. ; Pandis, Spyros N. *Atmospheric Chemistry and Physics - From Air Pollution to*  
701 *Climate Change (2nd Edition)*. John Wiley & Sons, accessed November 2013, 2006

702 Simpson W.R., von Glasow, R., Riedel K., Anderson P., Ariya P., Bottenheim J., Burrows J., Carpenter  
703 L. J., Friess U., Goodsite M. E., Heard D., Hutterh M., Jacobi H.-W., Kaleschke L., Neff B., Plance J.,  
704 Platt U., Richter A., Roscoe H., Sander R., Shepson P., Sodeau J., Steffen A., Wagner T., and Wolff E.:  
705 Halogens and their role in polar boundary-layer ozone depletion, *Atmos. Chem. Phys.*, 7, 4375–4418,  
706 2007.

707 Vogt R., Crutzen P. J., and Sander R.: A mechanism for halogen release from sea-salt aerosol in the  
708 remote marine boundary layer, *Nature*, 383, 327-330, 1996.

709 Von Glasow R. and Sander R.: Variation of sea salt aerosol pH with relative humidity, *Geophysical*  
710 *Research Letters*, 28, 2, 247-250, 2001.

711 Von Glasow R., Sander R., Bott, A., Crutzen P. J.: Modeling halogen chemistry in the marine boundary  
712 layer 1. Cloud-free MBL, *Journal of Geophysical Research* 107, D17, 4341,  
713 doi:10.1029/2001JD000942, 2002.

714 Von Glasow R., von Kuhlmann R., Lawrence M. G., Platt U., and Crutzen P. J.: Impact of reactive  
715 bromine chemistry in the troposphere, *Atmos. Chem. Phys.*, 4, 2481-2497, 2004.

716 Von Glasow, R.: Atmospheric Chemistry in Volcanic Plumes, *PNAS*, 107, 15, 6594-6599, 2010.

717 Wachsmuth M., Gäggeler H. W., von Glasow R., Ammann M. : Accommodation coefficient of HOBr  
718 on deliquescent sodium bromide aerosol particles, *Atmos. Chem. Phys.*, 2, 121–131, 2002.

719 Wang T. X. and Margareem D. W.: Kinetics of Reversible Chlorine Hydrolysis: Temperature  
720 Dependence and General-Acid/ Base-Assisted Mechanisms, *Inorg. Chem.*, 33, 1050-1055, 1994.

721 Wexler A. S. and Clegg S. L.: Atmospheric aerosol models for systems including the ions  $H^+$ ,  $NH_4^+$ ,  $Na^+$ ,  
722  $SO_4^{2-}$ ,  $NO_3^-$ ,  $Cl^-$ ,  $Br^-$  and  $H_2O$ . *J. Geophys. Res.* 107, No. D14, 4207-4220, 2002.

723 Wilson, T.R.S.: Salinity and the major elements of sea water. In: Riley, J.P., Skirrow, G. (Eds.),  
724 *Chemical Oceanography* (1, 2 Edition). Academic, Orlando FL, 365 – 413, 1975.

725 Yang, X., Cox R. A., Warwick N. J., Pyle J. A., Carver G. D., O'Connor F. M., and Savage N. H.:  
726 Tropospheric bromine chemistry and its impacts on ozone: A model study, *J. Geophys. Res.*, 110,  
727 D23311, doi:10.1029/2005JD006244., 2005.

728

**Table 1. Summary of experimental data reported on HOBr uptake coefficient and HOBr<sub>(aq)</sub> reaction kinetics under tropospheric conditions.**

Aerosol or Solution	Temperature K	$k_{\text{ter}}$ $\text{M}^{-2} \text{s}^{-1}$	$k^{\text{I}}$ $\text{s}^{-1}$	$k^{\text{II}}$ $\text{M}^{-1} \text{s}^{-1}$	$\gamma_{\text{HOBr}}$	$\alpha_{\text{HOBr}}$	Ref.
<b>HOBr + Cl<sup>-</sup><sub>(aq)</sub></b>							
HCl-acidified NaCl aerosol with HCl:NaCl = 0.1:1	298	-	-	-	> 0.2	-	a
H <sub>2</sub> SO <sub>4</sub> -acidified sea-salt aerosol with H <sub>2</sub> SO <sub>4</sub> :NaCl = 1.45:1	296	-	10 <sup>3</sup>	-	10 <sup>-3</sup> -10 <sup>-2</sup>	-	b
BrCl <sub>(aq)</sub> solution, pH = 6.4	298	2.3·10 <sup>10</sup>	-	-	-	-	c
<b>HOBr+Br<sup>-</sup><sub>(aq)</sub></b>							
HOBr uptake onto supersaturated NaBr <sub>(aq)</sub> , Br <sup>-</sup> <sub>(aq)</sub> > 0.2 M, at very low [HOBr <sub>(g)</sub> ]	296 ±2	-	-	-	-	0.6	d
Br <sub>2(aq)</sub> solution, pH = 2.7-3.8	298	1.6·10 <sup>10</sup>	-	-	-	-	e
Br <sub>2(aq)</sub> solution, pH = 1.9-2.4	298	1.6(±0.2)·10 <sup>10</sup>	-	-	-	-	f

<sup>a</sup>Abbatt and Waschewsky (1998)

<sup>b</sup>Pratte and Rossi (2006)

<sup>c</sup>Liu and Margareem (2002)

<sup>d</sup>Wachsmuth et al. (2002)

<sup>e</sup>Eigen and Kustin (1962)

<sup>f</sup>Beckwith et al. (1996)

**Table 2. Extraction of second-order rate constant values,  $k^{\text{II}}$  from reported experimental data. For HOBr+Br,  $k^{\text{II}}$  is derived from reported termolecular rate constants using  $k^{\text{II}} = k_{\text{ter}} \cdot [\text{H}^+_{(\text{aq})}]$ . For HOBr+Cl-  $k^{\text{II}}$  is derived from a reported termolecular rate constant using  $k^{\text{II}} = k_{\text{ter}} \cdot [\text{H}^+_{(\text{aq})}]$  and from reported first-order rate constant data,  $k^{\text{I}}$  using  $k^{\text{II}} = k^{\text{I}} / [\text{Cl}^-_{(\text{aq})}]$ . Molarity and Activity of  $\text{Cl}^-_{(\text{aq})}$  and  $\text{H}^+_{(\text{aq})}$  were calculated using the E-AIM model at 298.15 K. See Methods.**

Experiment	T K	RH %	wt% H <sub>2</sub> SO <sub>4</sub>	pH	Cl <sup>-</sup> <sub>(aq)</sub> Activity M	k <sub>ter</sub> M <sup>-2</sup> s <sup>-1</sup>	k <sup>I</sup> s <sup>-1</sup>		k <sup>II</sup> M <sup>-1</sup> s <sup>-1</sup>		Ref.
							(α = 0.2 <sup>*</sup> )	(α = 0.02 <sup>*</sup> )	(α = 0.2 <sup>*</sup> )	(α = 0.02 <sup>*</sup> )	
<b>HOBr+Br<sup>-</sup></b>											
Br <sub>2(aq)</sub>	293	-	-	2.7-3.6	-	1.6·10 <sup>10</sup>	-	-	4·10 <sup>6</sup> - 3.2·10 <sup>7</sup>		a
Br <sub>2(aq)</sub>	298	-	-	1.9-2.4	-	1.6 (±0.2)·10 <sup>10</sup>	-	-	6.1·10 <sup>7</sup> - 1.9·10 <sup>8</sup>		b
<b>HOBr+Cl<sup>-</sup></b>											
BrCl <sub>(aq)</sub>	298	-	-	6.4	2.0	2.3·10 <sup>10</sup>	-	-	8.8·10 <sup>3</sup>		c
H <sub>2</sub> SO <sub>4</sub> :NaCl (1.45:1)	296	77	31.7	-0.84	0.056	-	922	1855	1.6·10 <sup>4</sup>	3.3·10 <sup>4</sup>	d
	296	79	30.00	-0.75	0.069	-	1050	2510	1.5·10 <sup>4</sup>	3.6·10 <sup>4</sup>	
	296	80	29.1	-0.71	0.076	-	1140	3010	1.5·10 <sup>4</sup>	3.9·10 <sup>4</sup>	
	296	85	24.2	-0.48	0.127	-	800	1485	6.3·10 <sup>3</sup>	1.2·10 <sup>4</sup>	
	296	90	17.7	-0.21	0.209	-	995	2355	4.8·10 <sup>3</sup>	1.1·10 <sup>4</sup>	
H <sub>2</sub> SO <sub>4</sub> :NaCl (1.45:1)NSS	296	77	31.7	-0.84	0.056	-	1960	44000	3.5·10 <sup>4</sup>	7.8·10 <sup>5</sup>	d
H <sub>2</sub> SO <sub>4</sub> :NaCl (1.45:1) RSS	296	77	31.7	-0.84	0.056	-	545	795	9.6·10 <sup>3</sup>	1.4·10 <sup>4</sup>	d
	296	79	30.00	-0.75	0.069	-	720	1225	1.0·10 <sup>4</sup>	1.8·10 <sup>4</sup>	
	296	80	29.1	-0.71	0.076	-	1090	2600	1.4·10 <sup>4</sup>	3.4·10 <sup>4</sup>	
	296	85	24.2	-0.48	0.127	-	815	1580	6.4·10 <sup>3</sup>	1.2·10 <sup>4</sup>	
	296	90	17.7	-0.21	0.209	-	710	1210	3.4·10 <sup>3</sup>	5.8·10 <sup>3</sup>	

<sup>a</sup>Termolecular rate constant reported by Eigen and Kustin (1962)

<sup>b</sup>Termolecular rate constant reported by Beckwith et al. (1996)

<sup>c</sup>Termolecular rate constant reported by Liu and Magarem (2001) for buffered aerosol containing Cl<sup>-</sup><sub>(aq)</sub> at pH = 6.4 at T = 298 K.

<sup>d</sup>First-order rate constant,  $k^{\text{I}}_{\text{rxn}}$  data reported by Pratte and Rossi (2005) for aerosol mixture at H<sub>2</sub>SO<sub>4</sub>:NaCl = 1.45, for laboratory sea-salt, natural sea-salt (nss) or recrystallised sea-salt (rss). Pratte and Rossi (2006) assumed two different accommodation coefficients (α = 0.2, α = 0.02) in the derivation of  $k^{\text{I}}_{\text{rxn}}$  values from their uptake experiments, the former being closest to α = 0.6 reported on NaBr<sub>(aq)</sub> aerosol by Wachsmuth et al. (2002).

**Table 3. Underlying rate constant data ( $k_1$ ,  $k_{-1}$ ,  $k_0$ ,  $k_H$ ) used in  $k^{\text{II}}$  parameterisations of Figure 1.**

	HOBr+Br	HOBr+Cl
$k_1, \text{M}^{-1} \text{s}^{-1}$	$5 \cdot 10^8$ <sup>b,a</sup>	$1.2 \cdot 10^4$ <sup>c</sup>
$k_{-1}, \text{s}^{-1}$	$5 \cdot 10^8$ <sup>b,a</sup>	$1.1 \cdot 10^4$ <sup>c</sup>
$k_0, \text{s}^{-1}$	$10^4$ <sup>a</sup>	$2 \cdot 10^1$ <sup>c</sup>
$k_H, \text{M}^{-1} \text{s}^{-1}$	$2 \cdot 10^{10}$ <sup>a</sup>	$2 \cdot 10^{10}$ <sup>c</sup>

a: estimated in this study

b: derived from Eigen and Kustin (1962)

c: derived from Kumar and Margerum (1987)

**Table 4 Predicted uptake coefficients compared to reported uptake on experimental aerosol**

\* Br<sup>-</sup> concentration prior to aerosol dehumidifying (reported reduction in volume during dehumidifying indicates actual concentration may be a factor of ~3 higher)

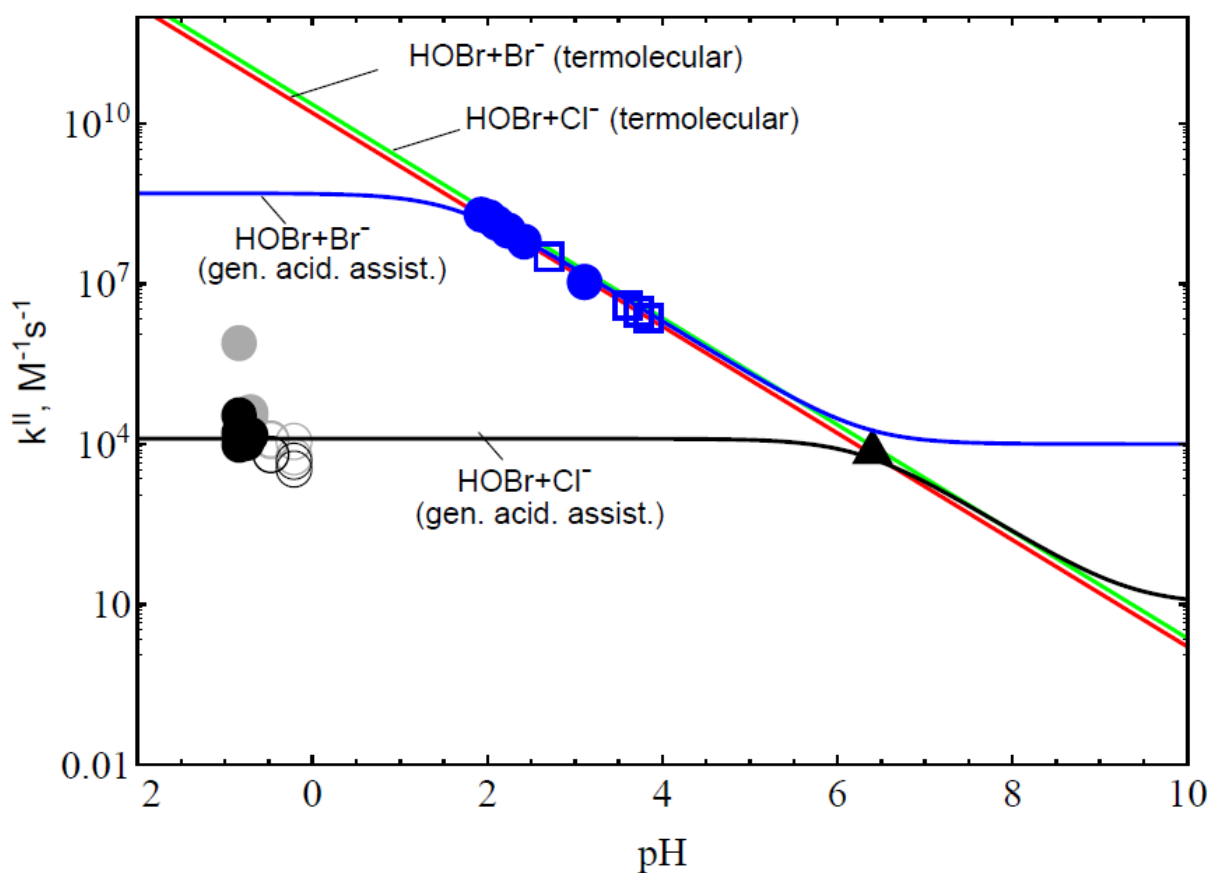
\*\* (reported modal radius, although particles >0.2 μm exist within the size spectrum)

Experimental aerosol:	NaBr aerosol (Wachsmuth et al., 2002) supersaturated NaBr <sub>(aq)</sub>	HCl-acidified NaCl aerosol (Abbatt and Waschewsky, 1998) HCl/NaCl = 0.1:1	H <sub>2</sub> SO <sub>4</sub> -acidified sea-salt aerosol (Pratte and Rossi, 2006) H <sub>2</sub> SO <sub>4</sub> /NaCl = 1.45:1	
γ <sub>H<sub>2</sub>OBr</sub> : observed	0.6 ± 0.2	> 0.2	(0.1-0.3)·10 <sup>-2</sup> at RH 40 to 70 %	(1.0±0.2)·10 <sup>-2</sup> at RH ≥ 76 %
<b>Uptake Model Parameters:</b>				
Temperature	298.15	298.15	298.15	298.15
α (accommodation coefficient)	0.6	0.6	0.6	0.6
Na concentration (μmol/m <sup>3</sup> )	-	0.2	0.8	0.8
RH, %	80	76	50	80
[Br <sup>-</sup> <sub>(aq)</sub> ], M	> 0.2*	-	-	-
[Cl <sup>-</sup> <sub>(aq)</sub> ], M (E-AIM)	-	6.6	4.4·10 <sup>-3</sup>	7.6·10 <sup>-2</sup>
[H <sup>+</sup> <sub>(aq)</sub> ], M (E-AIM)	~2·10 <sup>-6</sup>	2.3	83	5
pH	~6	-0.3	-1.9	-0.7
k <sup>ll</sup> , M <sup>-1</sup> s <sup>-1</sup>	3·10 <sup>4</sup>	10 <sup>4</sup>	10 <sup>4</sup>	10 <sup>4</sup>
k <sub>ter</sub> , M <sup>-2</sup> s <sup>-1</sup>	1.6·10 <sup>10</sup>	2.3·10 <sup>10</sup>	2.3·10 <sup>10</sup>	2.3·10 <sup>10</sup>
Particle radius, μm	>0.03**	1.	~0.17	~0.17
wt%H <sub>2</sub> SO <sub>4</sub>	-	-	48	29
H <sub>2</sub> OBr solubility, M atm <sup>-1</sup>	6.1·10 <sup>3</sup>	6.1·10 <sup>3</sup>	364	364
H <sub>2</sub> OBr Diffusion constant, cm <sup>2</sup> s <sup>-1</sup>	1.42·10 <sup>-5</sup>	1.42·10 <sup>-5</sup>	5.5·10 <sup>-6</sup>	1.0·10 <sup>-5</sup>
γ <sub>H<sub>2</sub>OBr</sub> : old approach (where k <sup>l</sup> = k <sub>ter</sub> ·[X <sup>-</sup> <sub>(aq)</sub> ]·[H <sup>+</sup> <sub>(aq)</sub> ])	0.1 < γ <sub>H<sub>2</sub>OBr</sub> ≤ 0.6	0.6	0.6	0.6
γ <sub>H<sub>2</sub>OBr</sub> : new approach (where k <sup>l</sup> = k <sup>ll</sup> ·[X <sup>-</sup> <sub>(aq)</sub> ])	0.1 < γ <sub>H<sub>2</sub>OBr</sub> ≤ 0.6	0.6	2·10 <sup>-4</sup>	7·10 <sup>-3</sup>

1 **Figure 1**

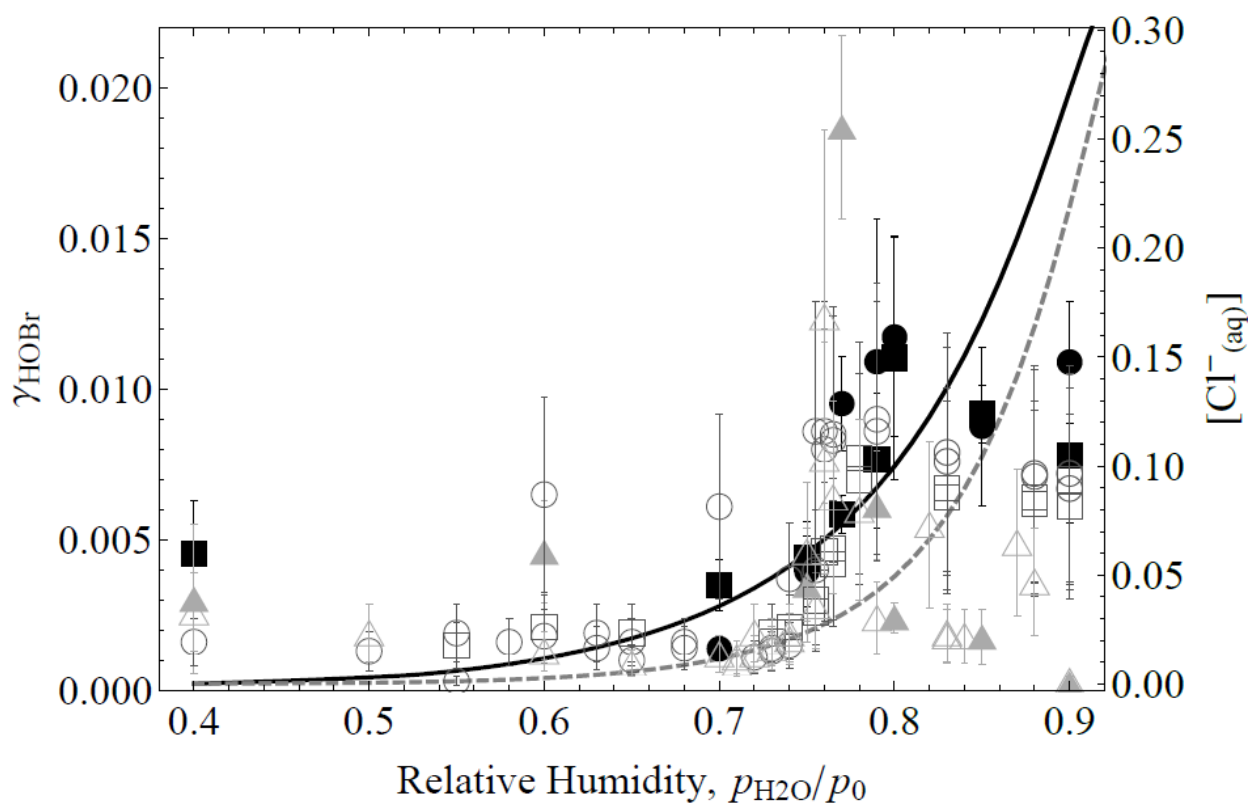
2 Second order rate constants for the reaction of HOBr with Br<sup>-</sup> and Cl<sup>-</sup> as a function of pH.  
3 Experimental estimates for k<sup>II</sup> for HOBr+Br<sup>-</sup> derived from data from Eigen and Kustin (1962) and  
4 Beckwith et al. (1996), (blue squares and circles respectively) are shown alongside model estimate  
5 (blue line) according to the acid-assisted mechanism. The red line denotes the k<sup>II</sup> rate constant  
6 assuming termolecular kinetics across all pH. Experimental estimates for k<sup>II</sup> for HOBr+Cl<sup>-</sup> derived  
7 from data from Liu and Margareem (2001) at pH = 6.4 (black triangle) and Pratte and Rossi (2006) at  
8 pH -1 to 0 (black and grey disks for data at RH = 77-80%, open circles for RH = 85-90%), are shown  
9 alongside model estimate (black line) according to the general acid-assisted mechanism. The green  
10 line denotes the k<sup>II</sup> rate constant assuming termolecular kinetics across all pH.

11



14 **Figure 2**

15 Dependence of reactive uptake coefficient for HOBr on relative humidity (RH) in the experiments of  
 16 Pratte and Rossi (2006) on H<sub>2</sub>SO<sub>4</sub>-acidified sea-salt aerosol (H<sub>2</sub>SO<sub>4</sub>:NaCl = 1.45:1) at 296 K, on  
 17 acidified sea-salt (circles), recrystallized sea-salt (squares) and natural sea-salt (triangles), under two  
 18 experimental set-ups: (i) the observed rate of HOBr<sub>(g)</sub> decay for a measured aerosol size distribution,  
 19 with effective radius ranging over 165-183 nm (filled shapes), and (ii) a survey type mode with HOBr  
 20 depletion monitored as a function of RH (unfilled shapes, with reported error estimated at 30-50%)  
 21 over a constant reaction time. Also shown is the modelled uptake coefficient for HOBr (black line),  
 22 and the Cl<sup>-</sup><sub>(aq)</sub> molarity (dotted line) as used within the uptake calculation.



23

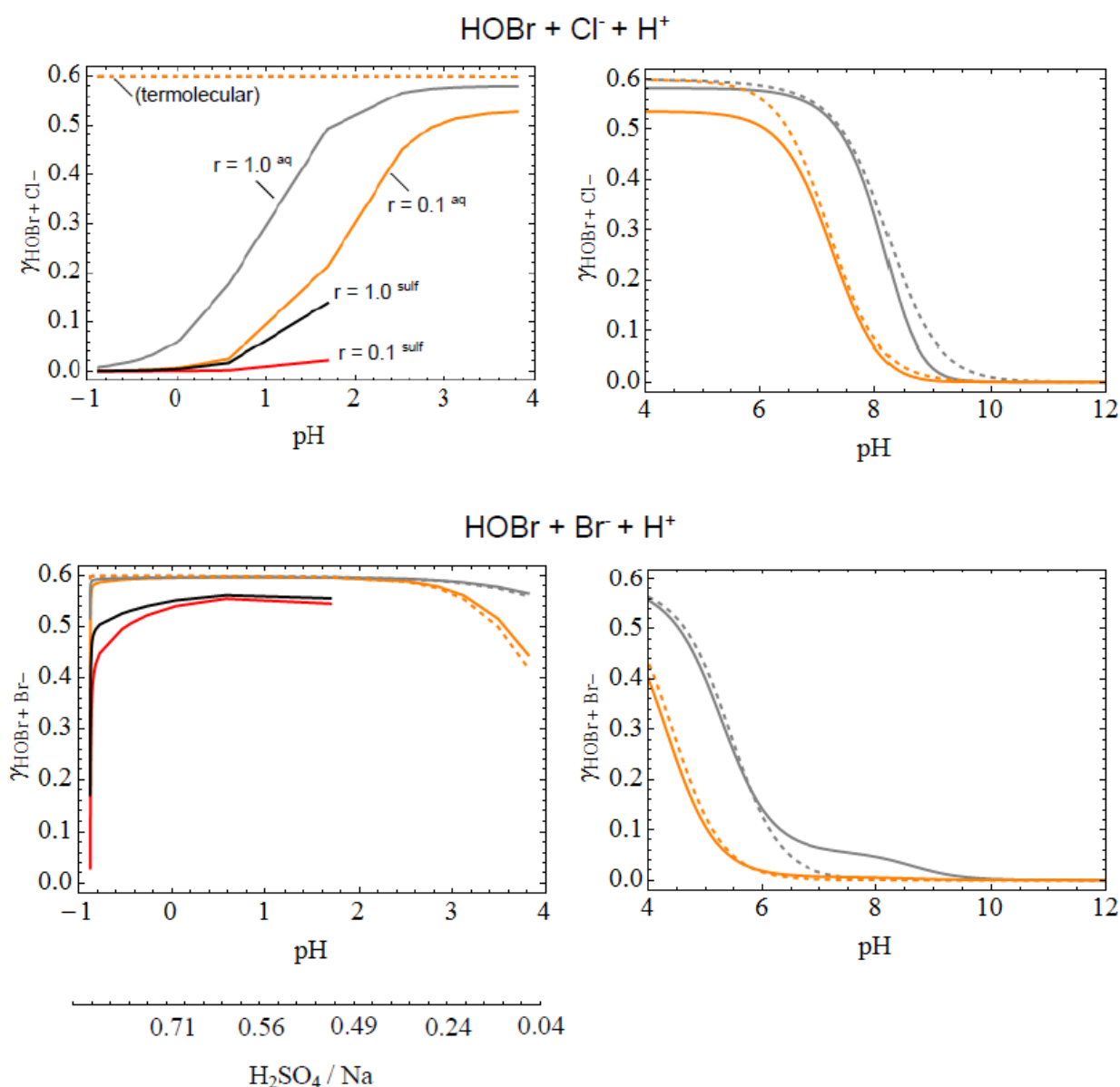
24

25



26 **Figure 3**

27 Variation in the HOBr uptake coefficient with pH, for reaction of HOBr with (upper) Cl<sup>-</sup> and (lower)  
 28 Br<sup>-</sup> on H<sub>2</sub>SO<sub>4</sub>-acidified sea-salt aerosol. Grey and orange lines denote uptake onto 1 and 0.1 μm  
 29 radius particles, respectively. Black and red lines denote uptake onto 1 and 0.1 μm radius particles  
 30 calculated using H<sup>+</sup> and D<sub>1</sub> parameterisations for sulfuric acid (rather than water), shown only for  
 31 H<sub>2</sub>SO<sub>4</sub>:Na ratios greater than 0.5. Relative humidity is set to 80% and Na concentration 1.3·10<sup>-7</sup>  
 32 moles/m<sup>3</sup> (equivalent to a PM10 of 10 μg/m<sup>3</sup> in the marine environment, Seinfeld and Pandis, 2006).  
 33 For comparison, uptake coefficients calculated assuming termolecular kinetics are also shown  
 34 (dashed lines).



35  
 36  
 37

38 **Figure 4**

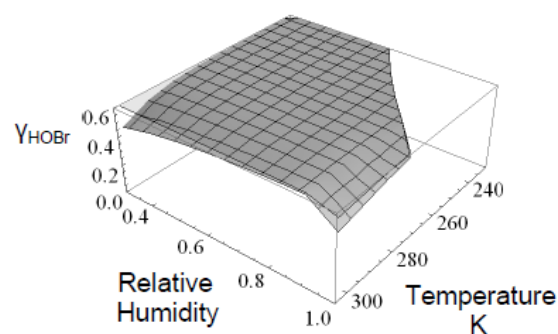
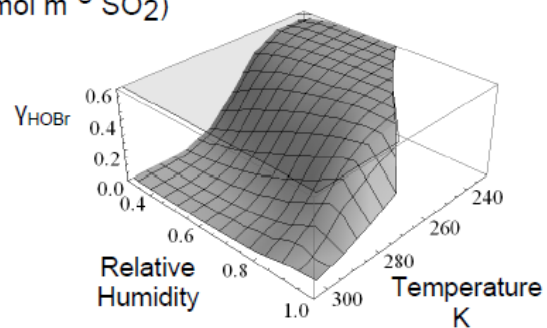
39 HOBr+Cl<sup>-</sup> and HOBr+Br<sup>-</sup> reactive uptake coefficients onto volcanic sulphate aerosol particles of 1 μm radius, calculated using our revised HOBr kinetics.  
40 Calculations are performed for a typical Arc or subduction zone volcanic plume composition containing a (SO<sub>2</sub>):HCl:H<sub>2</sub>SO<sub>4</sub>:HBr molar ratio mixture of  
41 1:0.5:0.01:0.00075. The plume strength is 30, or 0.3 μmol/m<sup>3</sup>, equivalent to approximately 1 or 0.01 ppmv SO<sub>2</sub> at 4 km altitude (US standard atmosphere).  
42 Conversely, uptake coefficients calculated using the termolecular approach yield high accommodation-limited values across all parameter space (light grey).

### HOBr+Cl<sup>-</sup>

### HOBr+Br<sup>-</sup>

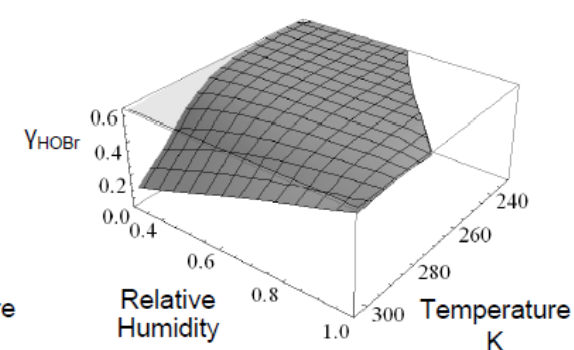
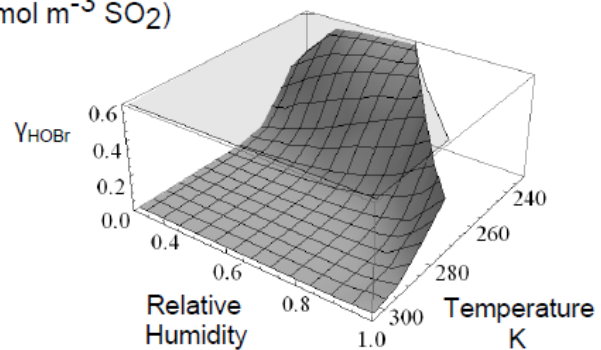
#### Strong plume

(30 μmol m<sup>-3</sup> SO<sub>2</sub>)



#### Weak plume

(0.3 μmol m<sup>-3</sup> SO<sub>2</sub>)



43

34